Modeling Volatility with Fractional Brownian Motion

Rémi Rehm
EDHEC Business School | Université Côte d'Azur

Juin 2023

I certify that the master project is my own research and I have properly acknowledge using brackets and a full bibliography all areas where I have drawn on the work, ideas and results of others and that the master project has not been presented to any other examination committee before and has not been published before.

Under supervision of :
M. François Delarue - Université Côte d'Azur
M. Florian Pelgrin - EDHEC Business School

Abstract

Matching volatility dynamics, term structure, and stylized facts such as long memory presents a modeling challenge. Modeling volatility in high-frequency data is particularly complex due to the specific market microstructure. Traditional stochastic volatility models are based on standard Brownian motion. In the groundbreaking article *Volatility is Rough* [10], the authors propose a model for high-frequency data volatility using stochastic processes driven by noisier signals than standard Brownian motion, specifically fractional Brownian motion with a Hurst parameter $H < 1/2$. This thesis firstly explores the mathematics of fractional Brownian motion and investigates Rough Paths integration through the Young's integral. The objective is, secondly, to develop the ability to simulate, test, and critically evaluate the model presented in the aforementioned article, the Rough Fractional Stochastic Volatility model.

Contents

Introduction

The theme of this research is volatility in finance. For a given asset, it is defined as the degree of variation of its price over time. Given the price series, volatility is usually measured by the standard deviation of logarithmic returns.

In market practices, the log-price P_t of a given asset usually follows the dynamic:

$$dP_t = \mu_t dt + \sigma_t dB_t$$

where $(\sigma_t)_{t\geq 0}$ is the volatility process. In the Black-Scholes framework, this is a constant. Then, models like Dupire's local volatility model [4] were developped to match exactly the prices of European options. They are called local volatility models. The problem is their unrealistic dynamics and that they generate off-market prices of exotic options. Stochastic volatility models were developped to price these exotic assets. For instance, we can cite the Hull and White model [9], the Heston model [8], and the SABR model [13]. In these models, volatility process is modeled by a continuous Brownian semi-martingale, that is to say stochastic volatility models offer volatility trajectories with smoothness close to that of Brownian motion.

An important and widely accepted stylized fact of market volatility is long-memory. The memory of a process and its regularity are two strongly linked caracteristics. It can be interesting to model volatility with processes featuring a wider range of regularity of the paths compared to standard Brownian motion.

The "smoothness" of the trajectories has been theorized in the 1990s by Terry Lyons [15] with his Rough Path Theory. Especially, it creates the appropriate framework to construct solutions of controlled differential equations driven by a highly oscillatory signal.

In 2014, Jim Gatheral, Thibault Jaisson and Mathieu Rosenbaum published the research paper *Volatility is Rough* [10]. It was a trendsetter in the finance industry. The article claims that volatility in high-frequency data follows "rougher" trajectories than standard Brownian motion. Actually, it uses an Ornstein-Uhlenbeck process to model log-volatility for a Hurst parameter $H < 1/2$. As part of a dual degree course in Finance and Applied Mathematics, I became interested in the question of this modeling and the mathematical tools used in this model, namely the construction of a stochastic integral with respect to fractional Brownian motion. With this perspective in mind, I began by asking whether volatility is indeed "rough" in the mathematical sense. In this thesis, after having defined the appropriate mathematical tools, I test whether this model is adequate.

So I started focusing on the required mathematical material to understand the model. I defined fractional Brownian motion and its main properties. Next, I dealt with fractional Ornstein-Uhlenbeck processes and I built a simulation algorithm. Finally, I tested the model.

Actually, in order to grasp what fractional Ornstein-Uhlenbeck process is and how to simulate it, we need to define an integral with respect to fractional Brownian motion. Much literature lingered over this question and we chose to introduce Young's integral which allows us to define an integral with respect to such trajectories with Hurst parameter $H > \frac{1}{2}$. These maths constitutes the two first sections of the thesis. Especially, the first part of the paper examines the fundamental properties of fractional Brownian motion. These properties play a crucial role in justifying its suitability as a tool for modeling high-frequency volatility in the later part of the paper. The second part utilizes the properties of fractional Brownian motion, such as Hölder continuity,

to explore the methodology for constructing the stochastic integral. In this section, Young's theorem is employed to define the stochastic integral pathway. The third chapter focuses on efficient simulation techniques for fractional Brownian motion, which is a vital tool for testing the model. The final section pertains to finance, where data is introduced and the model undergoes testing.

Additional proofs can be found in the **A. Additional Proofs** section.

1 Definitions and properties of fractional Brownian motion

This first part is dedicated to defining fractional Brownian motion, discussing its existence and introducing its initial properties. This insight will help us understand why we cannot construct an integral with respect to fractional Brownian motion in the same manner as we do with standard Brownian motion.

Definition 1. *A fractional brownian motion is the unique real-valued Gaussian process* $(B_t^H)_{t\in\mathbb{R}}$ *of mean 0 and of covariance function*

$$R_H(s,t) = \frac{V_H}{2}(|s|^{2H} + |t|^{2H} - |s-t|^{2H})$$

with

$$V_H = \frac{\Gamma(2-2H)cos(\pi H)}{\pi H(1-2H)}$$

when $H \neq 1/2$ *and equals 1 otherwise.*

Therefore the fractional Brownian motion is caracterized by the presence of long-term correlation. H is called the Hurst index and is the "memory" parameter. More precisely, $H > 1/2$ provides persistence which means that the trajectories tends to follow some trends and leads to smoother motion while $H < 1/2$ reveals noisier trajectories (see Firgure 1).

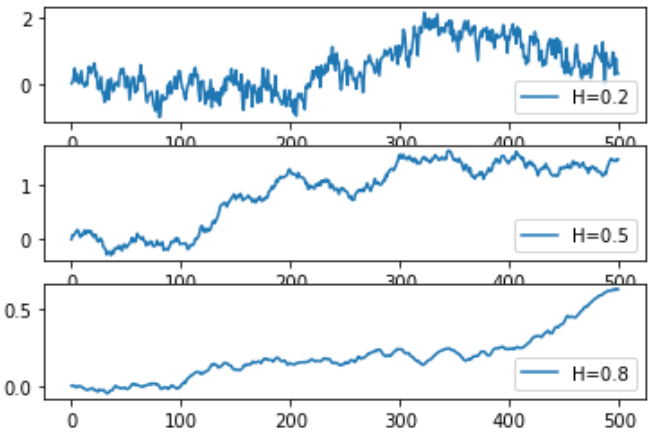

Figure 1: Simulated paths of fractional Brownian motion for different values of Hurst parameter.

We have obtained sample paths of fractional Brownian motion for different values of H thanks to the algorithm developped in section 3.

Fractional Brownian motion exhibits long memory increments when $H > 1/2$ in the sense that :

$$\sum_{n=0}^{+\infty} Cov(B_1^H, B_{n+1}^H - B_n^H) = +\infty$$

Proof.

$$\begin{aligned}
Cov(B_1^H, B_{n+1}^H - B_n^H) &= \frac{V_H}{2}\Big[|n-1|^{2H} - 2|n|^{2H} + |n+1|^{2H}\Big] \\
&= \frac{V_H n^{2H}}{2}\Big[\underbrace{(1-\frac{1}{n})^{2H}}_{1-\frac{2H}{n}+\frac{H(2H-1)}{n^2}+o(\frac{1}{n^2})} - 2 + \underbrace{(1+\frac{1}{n})^{2H}}_{1+\frac{2H}{n}+\frac{H(2H-1)}{n^2}+o(\frac{1}{n^2})} \Big] \\
&= \frac{V_H n^{2H}}{2}\Big[\frac{2H(2H-1)}{n^2} + o(\frac{1}{n^2})\Big] \\
&\sim V_H H(2H-1) n^{2H-2}
\end{aligned}$$

and because $\frac{1}{2} < H < 1$, the serie diverges. □

H is actually a parameter of control of the long-range dependance and then smoothness. From the above definition, Fractional Brownian motion satisfies self-similarity and has stationary increments :

Theorem 1. *Let $H \in (0,1)$. $(B_t^H)_{t\in\mathbb{R}}$ statisfies self-similarity that is $(B_{\alpha t}^H)_{t\in\mathbb{R}}$ follows the same law as $(\alpha^H B_t^H)_{t\in\mathbb{R}}$ for any positive α.*

Proof. $(B_{\alpha t}^H)_{t\in\mathbb{R}}$ and $(\alpha^H B_t^H)_{t\in\mathbb{R}}$ both are Gaussian processes of mean 0. It sufficies to prove that they have the same covariance function. For all $(s,t) \in \mathbb{R}^2$:

$$\begin{aligned}
Cov(\alpha^H B_t^H, \alpha^H B_s^H) &= \alpha^{2H}\frac{V_H}{2}(|s|^{2H} + |t|^{2H} + |s-t|^{2H}) \\
&= \frac{V_H}{2}(|\alpha s|^{2H} + |\alpha t|^{2H} + |\alpha s - \alpha t|^{2H}) \\
&= Cov(B_{\alpha t}^H B_{\alpha s}^H)
\end{aligned}$$

□

Theorem 2. *Fractional Brownian motion has stationary increments.*

Proof. By definition, a process $(X_t)_{t\in\mathbb{R}}$ is said to be stationary if :

$$\forall h > 0, \quad (X_{t+h})_{t\in\mathbb{R}} \sim (X_t)_{t\in\mathbb{R}}$$

Hence, we need to show that :

$$\forall h > 0,\ \forall (s,t) \in \mathbb{R}^2, \quad B_{s+h}^H - B_{t+h}^H \sim B_s^H - B_t^H$$

Let $h > 0$. But $B^H_{s+h} - B^H_{t+h}$ and $B^H_s - B^H_t$ are centered gaussian random variables and one has:

$$\begin{aligned}\mathbb{E}((B^H_s - B^H_t)^2) &= \mathbb{E}((B^H_s)^2) + \mathbb{E}((B^H_t)^2) - 2\mathbb{E}(B^H_t B^H_s) \\ &= V_H s^{2H} + V_H t^{2H} - V_H(t^{2H} + s^{2H} - |s-t|^{2H}) \\ &= V_H |s-t|^{2H} \\ &= V_H |(s+h) - (t+h)|^{2H} \\ &= \mathbb{E}((B^H_{s+h} - B^H_{t+h})^2)\end{aligned}$$

□

From the article of L. Decreusefond and A.S. Üstünel [3], there is also the following representation:

$$\forall t \in \mathbb{R}, \qquad B^H_t = \int_0^t K_H(t,s) dB_s$$

for some kernel measurable function K_H with $K_H(t,.)$ squared integrable, where B is the standard Brownian motion. Since K_H is a function of t, the fractional Brownian motion is probably not a semi-martingale and we cannot simply define an integral with respect to some fractional brownian motion as an integral with respect to a semi-martingale. Actually, we will prove in **2. Stochastic integral with respect to fractional Brownian motion** that fractional Brownian motion is not a semi-martingale once we have introduced the appropriate tools. For now, we must know that fractional Brownian motion does not satisfy independency of its increments in general:

Proof. For all $0 \leq s < t$,

$$\mathbb{E}((B^H_t - B^H_s)B^H_s) = \frac{V_H}{2}(|s|^{2H} + |t|^{2H} + |s-t|^{2H}) - V_H|s|^{2H} = \frac{V_H}{2}(-|s|^{2H} + |t|^{2H} + |s-t|^{2H})$$

Take t=2, s=1 and obtain :

$$\mathbb{E}((B^H_t - B^H_s)B^H_s) = V_H(2^{2H-1} - 1)$$

which equals zero iif $V_H = 0$ or $2^{2H-1} - 1 = 0$ iif $H = 1/2$. Hence B^H do not have independent increments. □

Actually, when H=1/2, B^H is a standard Brownian motion. Indeed, $B^{1/2}$ is a continuous Gaussian process of mean 0 with $B^{1/2}_0 = 0$ and for $0 < s < t$:

$$\mathbb{E}(B^{1/2}_t B^{1/2}_s) = \frac{V_{1/2}}{2}(t + s - |t-s|) = s = min(s,t)$$

since $V_{1/2} = 1$. Standard Brownian motion has independant increments. It explains why we obtained independancy of increments of fractional Brownian motion if and only if $H = 1/2$ in the previous proof. The independancy of increments of standard Brownian motion is the key property which allows us to build the Itô's stochastic integral. Thus, we cannot build the stochastic integral with respect to fractional Brownian motion as we did with respect to the standard Brownian motion and then with respect to semi-martingale.

The next theorem is a highly important property of fractional Brownian motion paths that will enable us to construct the integral subsequently.

Theorem 3. *The sample-paths of $(B_t^H)_{t\in\mathbb{R}}$ are almost-surely Hölder continuous of any order $\gamma < H$.*

Let us finish the first part with the existence of fractional Brownian motion. We know that if an application $m : \mathbb{R} \to \mathbb{R}$ and an application $c : \mathbb{R}^2 \to \mathbb{R}$ symmetrical and positive semi-definite exist, there is a Gaussian process of mean m and of covariance function c. Existence of such Gaussian process is a consequence of Kolmogorov extension theorem and the fact that the law of a Gaussian vector is defined by its mean and covariance. The uniqueness of the fractional Brownian motion is due to the fact that it has continuous trajectories. Proving that the covariance function R_H is symmetrical and positive semi-definite leads to the following theorem.

Theorem 4. *For any $H \in (0, 1)$, fractional Brownian motion of Hurst parameters H exists and is unique up to indistinguishability.*

2 Stochastic integral with respect to fractional Brownian motion

The objective of the second part is to give sense to what "fractional Ornstein-Uhlenbeck process" means. To do so, we need to understand what is an integral with respect to fractional Brownian motion. We will also add some new properties about smoothness of fractional Brownian motion trajectories.

2.1 Stieltjes integral

This section is dedicated to introduce the tools required to perform the Young's proof. We define Stieltjes integral and get some useful properties such as the caracterization of its existence that will be used at the end the Young theorem's proof and also Integration By Part theorem.

Let's begin with a definition :

Definition 2. *Recall that $\phi : J \to V$, J a compact interval and V a Banach space endowed with $|.|$ as a norm, has bounded variation if :*

$$sup_{\tau \subset J} \sum_{i=0}^{r-1} |\phi(t_{i+1}) - \phi(t_i)| < +\infty$$

where the supremum is taken over all the subdivisions τ of J.

This is a regularity condition. Graphically, a real-valued function is of bounded variation if the distance along the y-axis traveled by a point following the graph of the function is finite. A function which is continuous on an interval is not necessarly of bounded variation on the interval but a Lipschitz continuous function is of bounded variation. Besides, a function of bounded variation is bounded. Let's define now the Stieltjes integral.

Definition 3. *We define $S_\tau^\psi(f, \phi)$ the Riemann-Stieltjes sum as :*

$$S_\tau^\psi(f, \phi) := \sum_{i=1}^{m} f(\psi_i)[\phi(x_i) - \phi(x_{i-1})]$$

where $\tau = \{a = x_0 < ... < x_m = b\}$ is a subdivision and $\psi = (\psi_i)_{i=1,...,m}$ where $x_{i-1} < \psi_i < x_i$. If $S_\tau^\psi(f, \phi)$ converges as the mesh $|\tau| \to 0$, the limit is called the Stieltjes integral and is written $\int_a^b f(x)d\phi(x)$, that is :

$$\exists I \in V \quad \forall \epsilon > 0 \quad \exists \delta > 0 \quad \forall \tau, \psi \ : \quad |\tau| < \delta \implies |S_\tau^\psi(f, \phi) - I| < \epsilon$$

and one denotes $I := \int_a^b f(x)d\phi(x)$.

There is an important caracterisation of the existence of the Stieltjes integral which comes from the property of convergence of Cauchy sequences in Banach spaces :

Theorem 5. *$\int_a^b f(x)d\Phi(x)$ exists as a Stieltjes integral if and only if :*

$$\forall \epsilon > 0 \quad \exists \delta > 0 \quad \forall \tau, \tau' \ : \quad |\tau|, |\tau'| < \delta \implies |S_\tau^\psi(f, \phi) - S_{\tau'}^\psi(f, \phi)| < \epsilon$$

There also is an integration by part theorem for this integral:

Theorem 6. *If $\int_a^b f d\phi$ exists, then so does $\int_a^b \phi df$ and :*

$$\int_a^b f d\phi = [f(b)\phi(b) - f(a)\phi(a)] - \int_a^b \phi df$$

Proof. ([17]) Let $\tau = \{a = x_0 < \cdots < x_m = b\}$ a subdivision of $[a, b]$ and $\psi = (\psi_i)_{i=1,\ldots,m}$ such that $x_{i-1} < \psi_i < x_i$. One has :

$$\begin{aligned}
S_\tau^\psi(f,\phi) &= \sum_{i=1}^{m} f(\psi_i)\phi(x_i) - \sum_{i=0}^{m-1} f(\psi_{i+1})\phi(x_i) \\
&= -\sum_{i=1}^{m-1} \phi(x_i)[f(\psi_{i+1}) - f(\psi_i)] + f(\psi_m)\phi(b) - f(\psi_1)\phi(a) \\
&= -\Big[\underbrace{\sum_{i=1}^{m-1} \phi(x_i)[f(\psi_{i+1}) - f(\psi_i)] + \phi(a)(f(\psi_1) - f(a)) + \phi(b)(f(b) - f(\psi_m))}_{=:S_\sigma^{\tau'}(\phi,f)}\Big] \\
&\quad + \phi(b)f(b) - \phi(a)f(a)
\end{aligned}$$

with $\sigma = \{a = \sigma_0, \sigma_i = \psi_{i+1}, \sigma_m = b\}_{i=1,\ldots,m-1}$ and $\tau' = (x_i)_{i=1,\ldots,m}$. Because ψ straddle the x_i, $S_\sigma^{\tau'}(\phi, f)$ is a Riemann-Stieltjes sum. Therefore, observing that ϕ and f can be interchanged and taking the limit as $|\tau| \to 0$, we obtain the result. □

This last theorem provides an explicit computation of the Stieltjes integral with respect to functions of bounded variation. The proof can be found in [17].

Theorem 7. *([17]) If f is a continuous function and if ϕ has bounded variation, both defined on a bounded interval $[a, b]$, then the Stieltjes integral exists as :*

$$\int_a^b f(x)d\phi(x) = \lim_{n\to\infty} \sum_{i=0}^{p_n-1} f(t_i^n)[\phi(t_{i+1}^n) - \phi(t_i^n)]$$

for a given sequence of embedded subdivisions $\left\{a = t_0^n < t_1^n < \ldots < t_{p_n}^n = b\right\}$ of mesh that tends to 0 as $n \to \infty$.

This theorem provides a motivation to define the integral with respect to fractional Brownian motion "from one ω to the other" as the limit of $\sum_{i=0}^{p_n-1} f(t_i^n)[B_{t_{i+1}^n}^H(\omega) - B_{t_i^n}^H(\omega)]$ for a given $\omega \in \Omega$. The problem is that fractional Brownian motion paths are not of bounded variation. This is the topic of the next section.

2.2 p-Variation

In this section, we introduce the p-variation of a given trajectory and we prove that fractional Brownian motion has paths of unbounded variation. Furthermore, we will be equipped with all the tools to prove that fractional Brownian motion is not a semi-martingale in general which closes the previous debate of defining the integral with respect to fractional Brownian motion as a standard stochastic integral with respect to a semi-martingale.

Definition 4. *Let J a compact interval of $\mathbb{R}$, $p \geq 1$ a real number and $X : J \to E$ a E-valued continuous path on J, where E is a Banach space with norm $|.|$. For a given subdivision τ, let's denote :*

$$Var_p^\tau(X) := \sum_{j=0}^{r-1} |X_{t_j} - X_{t_{j+1}}|^p$$

Define the p-variation of X on J by:

$$\|X\|_{p,J} := [\sup_{\tau \subset J} Var_p^\tau(X)]^{\frac{1}{p}}$$

where supremum is taken over all the subdivisions of J. Let's denote $\nu_p(J, E)$ the subset of $C^0(J, E)$ of paths which have finite p-variation.

The following theorem will allow us to prove that fractional Brownian motion has sample-paths of unbounded variation.

Theorem 8. *([2]) Let B^H a fractional Brownian motion with $H \in]0, 1[$. For all $t \geq 0$, the random variable $Var_{1/H}^\tau(B^H)$ converges in norm $\mathbb{L}^2$ to $tV_H^{1/2H}\mathbb{E}(|N|^{\frac{1}{H}})$ as mesh $|\tau| \to 0$ where N is a standard gaussian random variable.*

Theorem 9. *Fractional Brownian motion has unbounded variation on any interval.*

Proof. Let us consider the sequence of subdivision $\tau = (\tau_n)_{n\in\mathbb{N}}$ where $\tau_n = \left\{0 = t_0 < ... < t_i = \frac{i}{n}t < ... < t_n = t\right\}$. From previous theorem, there is a subsequence of $(Var_{1/H}^{\tau_n}(B^H))_{n\in\mathbb{N}}$ such that for almost any $\omega \in \Omega$:

$$Var_{1/H}^{\tau_{n_k}}(B^H(\omega)) \xrightarrow[k\to\infty]{} tV_H^{1/2H}\mathbb{E}(|N|^{\frac{1}{H}}) \in]0, +\infty[$$

Moreover, one has for almost any $\omega \in \Omega$:

$$\begin{aligned} Var_{1/H}^{\tau_{n_k}}(B^H(\omega)) &= \sum_{i=0}^{n_k-1} |B^H_{\frac{i+1}{n_k}t}(\omega) - B^H_{\frac{i}{n_k}t}(\omega)|^{\frac{1}{H}} \\ &\leq \sup_{i=0,...,n_k-1} |B^H_{\frac{i+1}{n_k}t}(\omega) - B^H_{\frac{i}{n_k}t}(\omega)|^{\frac{1}{H}-1} \sum_{i=0}^{n_k-1} |B^H_{\frac{i+1}{n_k}t}(\omega) - B^H_{\frac{i}{n_k}t}(\omega)| \\ &\leq \sup_{|x-y|<\frac{1}{n_k}} |B_x^H(\omega) - B_y^H(\omega)|^{\frac{1}{H}-1} \times \sup_{\tau\subset[0,t]} \sum_{i=0}^{n-1} |B^H_{t_{i+1}}(\omega) - B^H_{t_i}(\omega)| \end{aligned}$$

Hence, almost surely :

$$\sup_{\tau\subset[0,t]} \sum_{i=0}^{n-1} |B^H_{t_{i+1}}(\omega) - B^H_{t_i}(\omega)| \geq \frac{Var_{1/H}^{\tau_{n_k}}(B^H(\omega))}{\sup_{|x-y|<\frac{1}{n_k}} |B_x^H(\omega) - B_y^H(\omega)|^{\frac{1}{H}-1}}$$

and by continuity $\sup_{|x-y|<\frac{1}{n_k}} |B_x^H(\omega) - B_y^H(\omega)|^{\frac{1}{H}-1}$ tends to zero as $k \to +\infty$ (since $B^H(\omega)$ is continuous for almost any $\omega \in \Omega$, $\frac{1}{H} - 1 > 0$ and $n_k \xrightarrow[k\to\infty]{} \infty$). Thus, for almost any ω, $t \to B_t^H(\omega)$ has unbounded variation on $[0, t]$. □

Therefore, we cannot apply **Theorem 7** to define the appropriate integral. The next theorem proves that fractional Brownian motion is not a semi-martingale.

Theorem 10. *Quadratic variation of the fractional Brownian motion is 0 if $H > \frac{1}{2}$ and is $+\infty$ if $H < \frac{1}{2}$. Fractional Brownian motion is a semi-martingale iif $H = \frac{1}{2}$.*

Proof. Consider a sequence of embedded subdivisions $\tau = (\tau^{(n)})_{n\in\mathbb{N}}$ of $[0,t]$ such that $\tau_0^{(n)} = 0$ and $\tau_{p_n}^{(n)} = t$ with a mesh $|\tau^{(n)}|$ that goes to 0. Let $S_t^{\tau^{(n)}} := \sum_{k=0}^{p_n-1}(B^H_{t_{k+1}} - B^H_{t_k})^2$.

$\underline{H > 1/2}$. One has :

$$\begin{aligned}
\mathbb{E}(S_t^{\tau^{(n)}}) &= \sum_{k=0}^{p_n-1} \mathbb{E}(B^H_{t_{k+1}} - B^H_{t_k})^2) \\
&= \sum_{k=0}^{p_n-1} V_H |t_{k+1} - t_k|^{2H} \\
&= V_H \sum_{k=0}^{p_n-1} |t_{k+1} - t_k|.|t_{k+1} - t_k|^{2H-1} \\
&\leq (\sup_{k\in\{0,\dots,p_n-1\}} |t_{k+1} - t_k|^{2H-1}) V_H \sum_{k=0}^{p_n-1} |t_{k+1} - t_k| \\
&= |\tau^{(n)}|^{2H-1} V_H \times t \xrightarrow[n\to\infty]{} 0 \quad \text{since } 2H-1 > 0
\end{aligned}$$

Hence, $S_t^{\tau^{(n)}} \xrightarrow{\mathbb{L}^1} 0$ and thus $S_t^{\tau^{(n)}} \xrightarrow{\mathbb{P}} 0$ ie quadratic variation of B^H is equal to 0 for $H > 1/2$. Now let us suppose B^H is a semi-martingale with a reductio ad absurdum so that:

$$B^H = M + V$$

where M is a local continuous martingale and V a BV process both starting from 0. Hence one has $< B^H >=< M >= 0$ and therefore,M^2 is a continuous local martingale starting from 0. By definition, there is a non decreasing sequence of stopping times $(T_n)_{n\in\mathbb{N}}$ diverging toward $+\infty$ almost surely such that $(M^2)^{T_n}$ is a martingale. Thus :

$$\forall (n,t) \in \mathbb{N}\times\mathbb{R}_+, \mathbb{E}(M^2_{min(t,T_n)}) = \mathbb{E}(M_0^2) = 0$$

Hence, $\forall (n,t) \in \mathbb{N}\times\mathbb{R}_+, M^2_{min(t,T_n)} = 0$ almost surely and therefore, letting $T_n \xrightarrow[n\to\infty]{} \infty$, M^2 is indiscernable from the null process, that is $B^H = V$ almost surely, i.e. B^H is a BV process.

$\underline{H < 1/2}$. Let $D_n := \sup_{\substack{0=t_0<\dots<t_n=t \\ n\geq 1}} \mathbb{E}(\sum_{k=0}^{n-1}(B^H_{t_{k+1}} - B^H_{t_k})^2)$ where the supremum is taken over all the subdivision of $[0,t]$. Hence is it greater than the sum over the dyadic subdivision $0 = t_0^{(n)} < \dots < t_i^{(n)} < \dots < t_{2^n}^{(n)} = t$, where $t_i^{(n)} = i2^{-n}t$:

$$\begin{aligned}
D_n &\geq \mathbb{E}(\sum_{k=0}^{2^n-1} (B^H_{t^n_{k+1}} - B^H_{t^n_k})^2) \\
&= \sum_{k=0}^{2^n-1} V_H |t_{k+1} - t_k|^{2H} \\
&= V_H 2^n |\frac{t}{2^n}|^{2H} = V_H |t|^{2H} 2^{n(1-2H)} \xrightarrow[n\to\infty]{} +\infty \quad \text{since } 1-2H > 0
\end{aligned}$$

Hence, $\sum_{k=0}^{n-1}(B^H_{t_{k+1}} - B^H_{t_k})^2 \xrightarrow{\mathbb{L}^1} +\infty$ and thus $\sum_{k=0}^{n-1}(B^H_{t_{k+1}} - B^H_{t_k})^2 \xrightarrow{\mathbb{P}} +\infty$ that is quadratic variation of B^H diverges. Therefore, B^H is not a semi-martingale because otherwise, quadratic variation would only be defined on 0 which is in contradiction with continuity hypothesis. □

This latter theorem really drives the point home. It highlights the need for a novel approach to obtain an integral with respect to fractional Brownian motion. The Rough Paths theory will help shed some light on this question.

2.3 Young integral

In [15], authors use the following notation for X and Y two real valued functions on a compact interval $[0,T]$, and $\tau := \{0 = t_0 < ... < t_r = T\}$ a subdivision of $[0,T]$. Denote :

$$\int_\tau Y dX := \sum_{i=0}^{r-1} Y_{t_i}(X_{t_{i+1}} - X_{t_i})$$

Remark that if $\int_\tau Y dX$ converges as mesh of τ tends to 0, $\int_0^T Y_s dX_s$ exists as Stieltjes integral. This is because $\int_\tau Y dX$ is a Riemann-Stieltjes sum. Indeed, if $\tau = \{0 = t_0 < ... < t_r = T\}$, one has :

$$\int_\tau Y dX = S^\psi_\tau(f,\phi) \qquad \text{with } \psi = (t_i)_{i=0,...,r-1}$$

Therefore we have already defined the convergence of $\int_\tau Y dX$ and even given a characterization of this convergence in theorem.

Moreover, we have seen in **theorem 7** that Stieltjes integral is well defined for a path X of bounded variation but Young proved that if we have certain regularity on Y, $\int_0^T Y_s dX_s$ still exists when X has unbounded variation.

Theorem 11. *([15]) Let V and W two Banach spaces and denote $\mathcal{L}(V,W)$ the set of linear applications from V to W. Let $p, q \geq 1$ be two real numbers such that $\frac{1}{p} + \frac{1}{q} > 1$ and $T \in \mathbb{R}^*_+$. Consider $X \in \nu_p([0,T],V)$ and $Y \in \nu_q([0,T],\mathcal{L}(V,W))$. Then :*

$$\lim_{mesh\ |\tau|\to 0,\ \tau\subset[0,t]} \int_\tau Y dX$$

exists for any $t \in [0,T]$ and belongs to $\nu_p([0,T],W)$.

Proof. Let's perform the proof with X and Y to be respectively $\frac{1}{p}$- and $\frac{1}{q}$-Hölder continuous. It is a stronger assumption but it is consistent with the theorem since a $\frac{1}{p}$-Hölder continuous path has finite p-varition.
First, consider a partition of $[0,T]$ in $r+1$ points, $r \geq 2$, $\tau = \{0 = t_0 < ... < t_r = T\}$. There is an index $i_0 \in [\![1, r-1]\!]$ such that :

$$t_{i_0+1} - t_{i_0-1} \leq \frac{2}{r-1}T$$

Indeed, otherwise we would have :

$$\begin{cases} t_2 - t_0 > \frac{2}{r-1}T \\ t_3 - t_1 > \frac{2}{r-1}T \\ ... \\ t_r - t_{r-2} > \frac{2}{r-1}T \end{cases}$$

and by summing :

$$t_r + t_{r-1} - t_1 - t_0 > (r-2+1)\frac{2}{r-1}T$$

that is :

$$t_{r-1} - t_1 > T$$

which is impossible.

The first step is to remove this index from the subdivision and to compute :

$$\begin{aligned}
&\Big|\int_\tau YdX - \int_{\tau-\{t_{i_0}\}} YdX\Big| \\
&= \Big|\Big[Y_{t_0}(X_{t_1}-X_{t_0}) + ... + Y_{t_{i_0-1}}(X_{t_{i_0}}-X_{t_{i_0-1}}) + Y_{t_{i_0}}(X_{t_{i_0+1}}-X_{t_{i_0}}) + Y_{t_{i_0+1}}(X_{t_{i_0+2}}-X_{t_{i_0+1}}) + ... + Y_{t_{r-1}}(X_{t_r}-X_{t_r})\Big] \\
&- \Big[Y_{t_0}(X_{t_1}-X_{t_0}) + ... + Y_{t_{i_0-2}}(X_{t_{i_0-1}}-X_{t_{i_0-2}}) + Y_{t_{i_0-1}}(X_{t_{i_0+1}}-X_{t_{i_0-1}}) + Y_{t_{i_0+1}}(X_{t_{i_0+2}}-X_{t_{i_0+1}}) + ... + Y_{t_{r-1}}(X_{t_r}-X_{t_r})\Big]\Big| \\
&= \Big|Y_{t_{i_0-1}}(X_{t_{i_0}}-X_{t_{i_0-1}}) + Y_{t_{i_0}}(X_{t_{i_0+1}}-X_{t_{i_0}}) - Y_{t_{i_0-1}}(X_{t_{i_0+1}}-X_{t_{i_0-1}})\Big| \\
&= \Big|Y_{t_{i_0-1}}X_{t_{i_0}} - \cancel{Y_{t_{i_0-1}}X_{t_{i_0-1}}} + Y_{t_{i_0}}X_{t_{i_0+1}} - Y_{t_{i_0}}X_{t_{i_0}} - Y_{t_{i_0-1}}X_{t_{i_0+1}} + \cancel{Y_{t_{i_0-1}}X_{t_{i_0-1}}}\Big| \\
&= \Big|(Y_{t_{i_0}} - Y_{t_{i_0-1}})(X_{t_{i_0+1}} - X_{t_{i_0}})\Big| \\
&\leq \|Y\|_{1/q}|t_{i_0} - t_{i_0-1}|^{\frac{1}{q}} \times \|X\|_{1/p}|t_{i_0+1} - t_{i_0}|^{\frac{1}{p}} \quad \text{(Hölder continuity)} \\
&\leq \|Y\|_{1/q}\|X\|_{1/p}|t_{i_0+1} - t_{i_0-1}|^{\frac{1}{p}+\frac{1}{q}}
\end{aligned}$$

The last inequality holds since :

$$\frac{|t_{i_0} - t_{i_0-1}|^{\frac{1}{q}}|t_{i_0+1} - t_{i_0}|^{\frac{1}{p}}}{|t_{i_0+1} - t_{i_0-1}|^{\frac{1}{p}+\frac{1}{q}}} = \Big|\underbrace{\frac{t_{i_0} - t_{i_0-1}}{t_{i_0+1} - t_{i_0-1}}}_{\leq 1}\Big|^{\frac{1}{q}} \times \Big|\underbrace{\frac{t_{i_0+1} - t_{i_0}}{t_{i_0+1} - t_{i_0-1}}}_{\leq 1}\Big|^{\frac{1}{p}} \leq 1$$

Now, from what we have found before for this index we can establish that :

$$\Big|\int_\tau YdX - \int_{\tau-\{t_{i_0}\}} YdX\Big| \leq C_{p,q,T}\left(\frac{1}{r-1}\right)^{\frac{1}{p}+\frac{1}{q}} \qquad \text{with } C_{p,q,T} := \|Y\|_{1/q}\|X\|_{1/p}(2T)^{\frac{1}{p}+\frac{1}{q}}$$

Second step: remove another index i_1 to the previous subdivision. Using the same argument as before, one has :

$$\exists i_1 \in [\![1, r-1]\!] - \{i_0\} : t_{i_1+1} - t_{i_1-1} \leq \frac{2}{(r-1)-1}T$$

and with similar calculation :

$$\begin{aligned}
\Big|\int_{\tau-\{t_{i_0}\}} YdX - \int_{\tau-\{t_{i_0},t_{i_1}\}} YdX\Big| &\leq \|Y\|_{1/q}\|X\|_{1/p}|t_{i_1+1} - t_{i_1-1}|^{\frac{1}{p}+\frac{1}{q}} \\
&\leq C_{p,q,T}\left(\frac{1}{r-2}\right)^{\frac{1}{p}+\frac{1}{q}}
\end{aligned}$$

Continue this process until there are 2 points left :

$$\left| \int_{\tau - \left\{ t_{i_0}, t_{i_1}, ..., t_{i_{r-3}} \right\}} Y dX - \int_{\tau - \left\{ t_{i_0}, t_{i_1}, ..., t_{i_{r-2}} \right\}} Y dX \right| \leq C_{p,q,T} \left(\frac{1}{(r-1)-(r-2)} \right)^{\frac{1}{p}+\frac{1}{q}}$$

We can now sum over all the inequalities and, using triangular inequality of the Banach space's norm, obtain:

$$\begin{aligned} \left| \int_{\tau} Y dX - \int_{\tau - \left\{ t_{i_0}, t_{i_1}, ..., t_{i_{r-2}} \right\}} Y dX \right| &\leq \sum_{k=0}^{r-2} C_{p,q,T} \frac{1}{(r-1-k)^{\frac{1}{p}+\frac{1}{q}}} \\ &= C_{p,q,T} \sum_{h=1}^{r-1} \frac{1}{h^{\frac{1}{p}+\frac{1}{q}}} \end{aligned}$$

Next, with $\frac{1}{p} + \frac{1}{q} > 1$, one obtains:

$$\left| \int_{\tau} Y dX - \underbrace{\int_{\tau - \left\{ t_{i_0}, t_{i_1}, ..., t_{i_{r-2}} \right\}} Y dX}_{= Y_0 (X_T - X_0)} \right| \leq C_{p,q,T} \underbrace{\zeta\left(\frac{1}{p} + \frac{1}{q} \right)}_{< +\infty}$$

where ζ is the standard Riemann zeta-function. Therefore, one has :

$$\begin{aligned} \left| \int_{\tau} Y dX \right| &\leq |Y_0 (X_T - X_0)| + C_{p,q,T} \zeta\left(\frac{1}{p} + \frac{1}{q} \right) \\ &\leq \|Y\|_\infty \|X\|_{1/p} |T-0|^{1/p} + \|Y\|_{1/q} \|X\|_{1/p} (2T)^{\frac{1}{p}+\frac{1}{q}} \zeta\left(\frac{1}{p} + \frac{1}{q} \right) \\ &\leq C(\|Y\|_\infty + \|Y\|_{1/q}) \|X\|_{1/p} \end{aligned}$$

where C is a finite constant which depends on T, p and q. Finally, taking the supremum over all the subdivisions of $[0, T]$, we obtain :

$$\sup_{\tau \subset [0,T]} \left| \int_{\tau} Y dX \right| \leq C(\|Y\|_\infty + \|Y\|_{1/q}) \|X\|_{1/p} \qquad (\triangle)$$

Next, consider a sequence $(X(n))_{n \in \mathbb{N}}$ of $\frac{1}{p}$-Hölder continuous paths with bounded variation. Therefore, for any $n \in \mathbb{N}$, $X(n) - X$ is $\frac{1}{p}$-Hölder continuous and assume that the sequence $(C_p^n)_{n \in \mathbb{N}}$ of Hölder constants satisfying :

$$\forall n \in \mathbb{N},\ \forall (s,t) \in \mathbb{R}_+^2 \ : \qquad |(X_t(n) - X_t) - (X_s(n) - X_s)|^p \leq C_p^n |t-s|$$

converges to 0 as $n \to \infty$.
Next, apply $X(n) - X$ to $(\triangle)$. Let $n \in \mathbb{N}$, one has:

$$\sup_{\tau \subset [0,T]} \left| \int_{\tau} Y d\left\{ X(n) - X \right\} \right| \leq C(\|Y\|_\infty + \|Y\|_{1/q}) C_p^n$$

Moreover,one has :

$$\begin{aligned}\int_\tau Y d\{X(n)-X\} &= \sum_{i=0}^{r-1} Y_{t_i}[(X_{t_{i+1}}(n)-X_{t_{i+1}})-(X_{t_i}(n)-X_{t_i})] \\ &= \sum_{i=0}^{r-1} Y_{t_i}[(X_{t_{i+1}}(n)-X_{t_i}(n))-(X_{t_{i+1}}-X_{t_i})] \\ &= \int_\tau Y dX(n) - \int_\tau Y dX\end{aligned}$$

from which we obtain :

$$\sup_{\tau\subset[0,T]}\left|\int_\tau Y dX(n) - \int_\tau Y dX\right| \xrightarrow[n\to\infty]{} 0$$

Furthermore, for each $n \geq 0$, $X(n)$ has bounded variation. Hence, from theorem 5 :

$$\lim_{|\tau|\to 0}\int_\tau Y dX(n) = \int_0^T Y_u dX_u(n)$$

exists as Stieltjes integral. To conclude the proof, from theorem 4, there is just to show that:

$$\forall\epsilon>0 \quad \exists\delta>0 \quad \forall\tau,\tau' : \quad |\tau|,|\tau'|<\delta \implies |\int_\tau Y dX - \int_{\tau'} Y dX| < \epsilon$$

Let $\epsilon > 0$. There is a rank $N \in \mathbb{N}$ such that for any $n \geq N$ and any subdivision τ of $[0,T]$,

$$|\int_\tau Y dX(n) - \int_\tau Y dX| < \epsilon$$

Let $n \geq N$. One has:

$$\exists\eta_n>0 \quad \forall\tau \qquad (\quad |\tau|<\eta \implies |\int_\tau Y dX(n) - \int_0^T Y_u dX_u(n)| < \epsilon \quad)$$

Now let τ,τ' two subdivisions of $[0,T]$ with a mesh lower than η_n. Therefore, one has:

$$\begin{aligned}&|\int_\tau Y dX - \int_{\tau'} Y dX| \\ &\leq |\int_\tau Y dX - \int_\tau Y dX(n)| + |\int_\tau Y dX(n) - \int_0^T Y_u dX_u(n)| \\ &+ |\int_0^T Y_u dX_u(n) - \int_{\tau'} Y dX(n)| + |\int_{\tau'} Y dX(n) - \int_{\tau'} Y dX| \\ &< 4\epsilon\end{aligned}$$

□

From Theorem 3, the sample paths of fBm are almost-surely Hölder continuous for all $\gamma < H$. They have almost-surely finite p-variation for all $p > \frac{1}{H}$. Therefore, Young theorem applies to continuous process Y of finite q-variation with $q < \frac{1}{1-H}$. Let $(\tau^{(n)})_{n\in\mathbb{N}}$ a sequence of embedded subdivisions of $[0,t]$ of mesh going to 0. Therefore, the sequence of random variables

$$\int_{\tau^{(n)}} Y dB^H$$

converges almost-surely and we denote the limit by:

$$\int_0^t Y_s dB_s^H$$

2.4 fractional Ornstein-Uhlenbeck [14]

We can now consider stochastic differential equations with noisier solutions such as solutions driven by fractional Brownian motion for instance. Actually, only Rough Path theory developped by Lyons [15] yields existence and uniqueness for solution of SDE driven by fractional Brownian motion with a Hurst parameter $H \in [0, 1/2[$. Rough Path is the generalization of Young integration. However, as explained in [14], for fractional Ornstein-Uhlenbeck equation, we integrate highly regular functions. Therefore, we will consider fractional Ornstein-Uhlenbeck processes for any $H \in (0, 1)$. Let's begin with the following theorem :

Theorem 12. *For $-\infty \leq a < \infty$, $\lambda, \sigma > 0$ and almost every $\omega \in \Omega$:*

$$\forall t > a : \quad \int_a^t e^{\lambda u} dB_u^H(\omega)$$

exists as Stieltjes integral and is equal to :

$$e^{\lambda t} B_t^H(\omega) - e^{\lambda a} B_a^H(\omega) - \lambda \int_a^t e^{\lambda u} B_u^H(\omega) du$$

Proof. Let :

$$\tilde{B}_s^H = \begin{cases} s^{2H} B_{1/s}^H & \text{if } s \neq 0 \\ 0 & \text{if } s = 0 \end{cases}$$

$(\tilde{B}_t^H)_{t\in\mathbb{R}}$ is obviously a Gaussian process of mean and covariance function :

$$\begin{aligned} &\mathbb{E}(\tilde{B}_t^H) = 0 \\ &\mathbb{E}(\tilde{B}_t^H \tilde{B}_s^H) = \begin{cases} \frac{V_H}{2}(st)^{2H}(|\frac{1}{t}|^{2H} + |\frac{1}{s}|^{2H} - |\frac{1}{t} - \frac{1}{s}|^{2H}) & \text{if } s \neq 0, t \neq 0 \\ 0 & \text{otherwise.} \end{cases} \\ &\qquad = \frac{V_H}{2}(|s|^{2H} + |t|^{2H} + |s-t|^{2H}) = R_H(s,t) \end{aligned}$$

Hence $(\tilde{B}_t^H)_{t\in\mathbb{R}}$ is a fractional Brownian motion. Then we know that $(\tilde{B}_t^H)_{t\in\mathbb{R}}$ have almost-surely Höler continuous sample-paths of any order $\gamma < H$, i.e. :

$$\exists N \subset \Omega \text{ negligible}, \forall \omega \notin N, \forall t \in \mathbb{R} : \qquad \forall \gamma < H, |\tilde{B}_t^H(\omega) - \tilde{B}_0^H(\omega)| \leq C_\gamma(\omega)|t-0|^\gamma$$

Let $\beta < H$. $\exists \gamma$ s.t. $\beta < \gamma < H$. Then :

$$\frac{|\tilde{B}_t^H(\omega)|}{|t|^\beta} \leq C_\beta(\omega)|t|^{\gamma-\beta} \xrightarrow[t\to 0]{} 0$$

That is :

$$\forall \beta < H : \lim_{t\to 0} \frac{|t^{2H} B_{1/t}^H(\omega)|}{|t|^\beta} = 0$$

From a change of variable :

$$\forall \beta < H : \lim_{|t'|\to\infty} \frac{|B_{t'}^H(\omega)|}{|t'|^{2H-\beta}} = 0$$

Since $\beta < H \Leftrightarrow 2H - \beta > H$, one has equivalently:

$$\forall \gamma > H : \lim_{|t|\to\infty} \frac{|B_t^H(\omega)|}{|t|^{\gamma}} = 0$$

Therefore,

$$\forall t > a : \qquad \int_a^t B_u^H(\omega) e^{\lambda u} du$$

exists as a Riemann integral. But also, one has :

$$\forall t > a : \qquad \int_a^t B_u^H(\omega) e^{\lambda u} du = \frac{1}{\lambda} \int_a^t B_u^H(\omega) d\left\{x \mapsto e^{\lambda x}\right\}_u$$

That is $\int_a^t B_u^H(\omega) d\left\{x \mapsto e^{\lambda x}\right\}_u$ exists as Riemann-Stieltjes integral. Hence, from **Theorem 6**, the Riemann-Stieltjes integral $\int_a^t e^{\lambda u} dB_u^H(\omega)$ exists. Note that we gave sense to this integral for $H > \frac{1}{2}$ in the previous section with Young's theorem. Integration by part theorem also provides:

$$\begin{aligned}\int_a^t e^{\lambda u} dB_u^H(\omega) &= e^{\lambda t} B_t^H(\omega) - e^{\lambda a} B_a^H(\omega) - \int_a^t B_u^H(\omega) d\left\{x \mapsto e^{\lambda x}\right\}_u \\ &= e^{\lambda t} B_t^H(\omega) - e^{\lambda a} B_a^H(\omega) - \lambda \int_a^t e^{\lambda u} B_u^H(\omega) du\end{aligned}$$

□

From this previous theorem, we immediately obtain that :

$$t \mapsto \int_a^t e^{\lambda u} dB_u^H(\omega)$$

is continuous. We can now define what fractional Ornstein-Uhlenbeck process is.

Theorem 13. *The unique continuous function y that solves the equation :*

$$y(t) = \zeta(\omega) - \lambda \int_0^t y(s) ds + \sigma B_t^H(\omega) \qquad (E)$$

is given by :

$$y(t) = e^{-\lambda t}\left(\zeta(\omega) + \sigma \int_0^t e^{\lambda u} dB_u^H(\omega)\right), \quad t \geq 0$$

Proof. A continuous function y solves (E) if and only if :

$$z(t) := \int_0^t y(s) ds, \quad t \geq 0$$

solves the ODE :

$$z'(t) = -\lambda z(t) + \zeta(\omega) + \sigma B_t^H(\omega), \quad z(0) = 0$$

which unique solution is given by :

$$z(t) = e^{-\lambda t} \int_0^t e^{\lambda u}(\zeta(\omega) + \sigma B_u^H(\omega))du, \quad t \geq 0$$

Therefore, the unique continuous function y that solves (E) is given by :

$$\begin{aligned} y(t) &= -\lambda e^{-\lambda t} \int_0^t e^{\lambda u}(\zeta(\omega) + \sigma B_u^H(\omega))du + \zeta(\omega) + \sigma B_t^H(\omega), \quad t \geq 0 \\ &= -\lambda e^{-\lambda t}(\frac{\cancel{e^{\lambda t}} - 1}{\lambda})\zeta(\omega) - \sigma\lambda e^{-\lambda t} \int_0^t e^{\lambda u} B_u^H(\omega)du + \cancel{\zeta(\omega)} + \sigma B_t^H(\omega) \end{aligned}$$

From previous theorem, one has :

$$\int_0^t e^{\lambda u} B_u^H(\omega)du = \frac{1}{\lambda}\left(e^{\lambda t} B_t^H(\omega) - \int_0^t e^{\lambda u} dB_u^H(\omega)\right)$$

Therefore, the unique solution y is given by :

$$\begin{aligned} y(t) &= e^{-\lambda t}\zeta(\omega) - \sigma e^{-\lambda t}\left(e^{\lambda t} B_t^H(\omega) - \int_0^t e^{\lambda u} dB_u^H(\omega)\right) + \sigma B_t^H(\omega) \\ &= e^{-\lambda t}\left(\zeta(\omega) + \sigma \int_0^t e^{\lambda u} dB_u^H(\omega)\right) \end{aligned}$$

□

From the last theorem, when choosing $\zeta(\omega) := \sigma \int_{-\infty}^0 e^{\lambda u} dB_u^H(\omega)$ provides the solution :

$$y(t) = \sigma \int_{-\infty}^t e^{-\lambda(t-u)} dB_u^H(\omega), \qquad t \geq 0$$

Actually, y is a realization of a solution of a particular case of the Langevin equation :

$$X_t = \zeta - \lambda \int_0^t X_s ds + N_t$$

where $(N_t)_{t\geq 0}$ is a noise process which can be more general than Brownian noise. Note that when $(N_t)_{t\geq 0}$ is $(\sigma B_t)_{t\geq 0}$ and $\zeta = X_0$ the initial condition, the Langevin equation is actually an Ornstein-Uhlenbeck equation.

Definition 5. *The unique solution $(Y_t^{H,\zeta})_{t\geq 0}$ of the Langevin equation with fractional Brownian noise $N_t = \sigma B_t^H$ is called fractional Ornstein-Uhlenbeck process with initial condition ζ.*

We actually solved the Langevin equation with fractional Brownian noise path-wise and found:

$$Y_t^{H,\zeta} = e^{-\lambda t}\left(\zeta + \sigma \int_0^t e^{\lambda u} dB_u^H\right), \quad t \geq 0$$

3 Simulation of fractional Brownian motion [7]

The objective of this chapter is to obtain an algorithm that is able to efficiently simulate sample paths of fractional Brownian motion on a finite time grid. It will allow us then to produce paths of fractional Ornstein-Uhlenbeck process. The mathematical development and results that follows are based on the exercise sheet of Paul P. Hager [7].

3.1 Simulation of Gaussian processes

Let $I \subset \mathbb{R}$ an interval. In order to simulate a Gaussian process $(X_t)_{t\in I}$ on a time grid $t_0 < \cdots < t_n$ for some $n \in \mathbb{N}$, the idea is to simulate the Gaussian (n+1)-dimensional Gaussian random variable $X := (X_{t_0}, \ldots, X_{t_n})$. To build an algorithm, let's use the following theorem:

Theorem 14. *(Cholesky decomposition) Let Σ positive semi-definite symmetric matrix. There exists a unique lower triangular matrix L such that:*

$$\Sigma = LL^T$$

Regarding the computation of the Cholesky decomposition, one can use the fact that L is lower triangular to compute its entries iteratively from the top to the bottom in the following way:

Algorithm 1 Provide the lower triangular matrix component of Cholesky decomposition

Require: $A \in \mathcal{S}_n^{++}(\mathbb{R})$, $n \geq 1$
  $L \leftarrow 0 \in \mathcal{M}_n(\mathbb{R})$
  for $i = 1$ up to n **do**
    for $j = 1$ up to i **do**
      $S \leftarrow$ scalar product of i^{th} and j^{th} row of L
      if $i = j$ **then**
        $L_{i,j} \leftarrow \sqrt{A_{i,i} - S}$
      else
        $L_{i,j} \leftarrow (A_{i,j} - S)/L_{j,j}$
      end if
    end for
  end for
  Return L

Let $Z_1, \ldots, Z_n$ be i.i.d standard normal random variables and consider the random vector $Z := (Z_1, \ldots, Z_n)$ which has multivariate Gaussian distribution.
Given a matrix $A \in \mathcal{M}_{m,n}(\mathbb{R})$ and $\mu \in \mathcal{M}_{m,1}(\mathbb{R})$. One knows that:

$$\mu + AZ \sim \mathcal{N}(\mu, AA^T)$$

Therefore, we can simulate the gaussian vector using the following algorithm :

Note that we can use the Box-Muller transform to simulate the iid sample of the standard normal random variables $(Z_1, \ldots, Z_n)$ or simply use the corresponding package.

3.2 Efficient simulation of certain stationary Gaussian processes

The computational effort of Algorithm 2 to generate m sample paths of a Gaussian process on a grid of size n is of the order $O(n^3) + mO(n^2)$, the first term appearing is from the computation of

Algorithm 2 Simulate a multivariate Gaussian random variable

Require: $\Sigma \in \mathcal{S}_n^{++}(\mathbb{R})$ the covariance matrix, $\mu \in \mathbb{R}^n$ mean vector, $m \in \mathbb{N}$ number of samples
  Compute L such that $\Sigma = LL^T$ using Algorithm 1
  for $i = 1$ up to m **do**
    Simulate n independant samples from the standard normal distribution $Z = (Z_1, \dots, Z_n)$
    Save new sample $\mu + LZ$
  end for

the Cholesky decomposition and the second term is from the matrix multiplication LZ with the standard Gaussian vector Z. We are now looking for a more efficient algorithm that simulates certain stationary Gaussian processes. The maths that come next are partly from [7]. The objective is to deliver a more efficient algorithm which will allow us to process a higher quantity of data. First, note the following theorem:

Theorem 15. *A Gaussian process $X = (X_t)_{t\in\mathbb{R}}$ is stationary if and only if the mean $\mathbb{E}(X_t)$ is constant and the covariance function C satisfies :*

$$C(s,t) = C(0, t-s)$$

Proof. Suppose X is stationary. For any $t \in \mathbb{R}$, $\tau \in \mathbb{R}$, $\mathbb{E}(X_t) = \mathbb{E}(X_{t+\tau})$ and moreover $Cov(X_s, X_t) = Cov(X_{s+\tau}, X_{t+\tau})$, hence choose $\tau = -s$ to get $C(s,t) = C(0, t-s)$. Fix now $(t_1, \dots, t_n) \in \mathbb{R}^n$ and $\tau \in \mathbb{R}$ and prove that $(X_{t_1}, \dots, X_{t_n}) \sim (X_{t_1+\tau}, \dots, X_{t_n+\tau})$. We only need to prove equality of mean (immediate) and covariance matrix but one has for any $i, j \in \{1, \dots, n\}$:

$$Cov(X_{t_i+\tau}, X_{t_j+\tau}) = Cov(X_0, X_{(t_i+\tau)-(t_j+\tau)}) = Cov(X_0, X_{t_i-t_j}) = Cov(X_{t_i}, X_{t_j})$$

□

Assume now that the time grid $(t_0, \dots, t_n) \subset \mathbb{R}$ is regular, that is there exists Δ such that $t_k = t_0 + k\Delta$ for any k. Consider the Gaussian vector $X := (X_{t_0}, \dots, X_{t_n})$ on the corresponding time grid with $X = (X_t)_{t\in\mathbb{R}}$ the corresponding Gaussian process of covariance function C and denote Σ its covariance matrix. Denote also $c_k := C(t_0, t_k)$ for any $k \in \{1, \dots, n\}$. Therefore, from previous theorem, one has:

$$\Sigma = \begin{pmatrix} c_0 & c_1 & \cdots & c_n \\ c_1 & \ddots & \ddots & \vdots \\ \vdots & \ddots & \ddots & c_1 \\ c_n & \cdots & c_1 & c_0 \end{pmatrix}$$

This is a Toeplitz matrix. Consider now the following matrix built from Σ by reflecting and shifting the first row :

$$\Pi = \begin{pmatrix} c_0 & c_1 & \cdots & c_{n-1} & c_n & c_{n-1} & \cdots & c_2 & c_1 \\ c_1 & c_0 & \cdots & c_{n-2} & c_{n-1} & c_n & \cdots & c_3 & c_2 \\ \vdots & \vdots & \ddots & \vdots & \vdots & \vdots & \ddots & \vdots & \vdots \\ c_{n-1} & c_{n-2} & \cdots & c_0 & c_1 & c_2 & \cdots & c_{n-1} & c_n \\ c_n & c_{n-1} & \cdots & c_1 & c_0 & c_1 & \cdots & c_{n-2} & c_{n-1} \\ c_{n-1} & c_n & \cdots & c_2 & c_1 & c_0 & \cdots & c_{n-3} & c_{n-2} \\ \vdots & \vdots & \ddots & \vdots & \vdots & \vdots & \ddots & \vdots & \vdots \\ c_1 & c_2 & \cdots & c_n & c_{n-1} & c_{n-2} & \cdots & c_1 & c_0 \end{pmatrix} \in \mathcal{M}_{2n,2n}(\mathbb{C})$$

This is a circulant matrix which can be conventionally written $C(c_0, c_1, \ldots, c_{n-1}, c_n, c_{n-1}, \ldots, c_2, c_1)$. If one denotes :

$$J := \begin{pmatrix} 0 & 1 & 0 & \cdots & \cdots & 0 \\ 0 & 0 & 1 & \ddots & & 0 \\ \vdots & & & \ddots & \ddots & \vdots \\ \vdots & & & & \ddots & 0 \\ 0 & & & & & 1 \\ 1 & 0 & 0 & \cdots & \cdots & 0 \end{pmatrix} \in \mathcal{M}_{2n,2n}(\mathbb{C}),$$

one has that $J = C(0, 1, \ldots, 0)$ and obtains immediately that :

$$\begin{cases} J^2 = C(0, 0, 1, \ldots, 0) \\ J^3 = C(0, 0, 0, 1, \ldots, 0) \\ \ldots \\ J^{2n} = I_{2n,2n} \quad \text{the identity matrix} \end{cases}$$

Therefore, $X^{2n} - 1$ is a canceling polynomial of J. Thus, the possible eigenvalues of J are the $2n^{th}$ roots of unity since we are considering a $\mathbb{C}$-vector space, for instance $\mathbb{C}^{2n}$. One can easily show that for any $k = 0, \ldots, 2n-1$, $\omega_n^k = e^{i\frac{k\pi}{n}}$ is an eigenvalue associated to the eigenspace:

$$E_k := Vect((1, \omega_n^k, \omega_n^{2k}, \ldots, \omega_n^{(2n-1)k}))$$

Therefore, J has $2n$ pairwise distinct eigenvalues and then, J is diagonalizable. Denote Ω the normalized transfer matrix from the canonical basis to the eigenvector basis so that :

$$J = \Omega \underbrace{\begin{pmatrix} 1 & & & & \\ & \omega_n & & & \\ & & \ddots & & \\ & & & \ddots & \\ & & & & \omega_n^{2n-1} \end{pmatrix}}_{D} \Omega^{-1}$$

with :

$$\Omega = \left(\frac{1}{\sqrt{2n}} \omega_n^{jk} \right)_{0 \leq j,k \leq 2n-1}$$

One proves easily by induction that :

$$\forall j \in [\![0, 2n-1]\!], \quad J^j = \Omega D^j \Omega^{-1}$$

which shows that all the J^j are diagonalizable with the same eigenvector basis as for J.
Now, from above computation, we remark that :

$$\Pi = \sum_{j=0}^{2n-1} \gamma_{j+1} J^j \qquad \text{where } \gamma = (c_0, c_1, \ldots, c_{n-1}, c_n, c_{n-1}, \ldots, c_2, c_1)$$

That is :

$$\Pi = \Omega \underbrace{\left(\sum_{j=0}^{2n-1} \gamma_{j+1} D^j \right)}_{\Delta} \Omega^{-1}$$

with :

$$\Delta = diag((\sum_{j=0}^{2n-1} \gamma_{j+1}\omega_n^{jk})_{k=0,\dots,2n-1})$$

Moreover, one has:

$$\Omega\Omega^* = I_{2n,2n}$$

Indeed, let $1 \leq p, q \leq 2n$:

$$\begin{aligned}(\Omega\Omega^*)_{p,q} &= \sum_{j=1}^{2n} \Omega_{p,j}\Omega^*_{j,q} \\ &= \frac{1}{2n}\sum_{j=1}^{2n} \omega_n^{(p-1)(j-1)}\bar{\omega_n}^{(j-1)(q-1)} \\ &= \frac{1}{2n}\sum_{j=1}^{2n} e^{i\frac{\pi}{n}(p-1)(j-1)}e^{-i\frac{\pi}{n}(j-1)(q-1)} \\ &= \frac{1}{2n}\sum_{j=1}^{2n} [e^{i\frac{\pi}{n}(p-q)}]^{(j-1)}\end{aligned}$$

Therefore, if $p = q$, $(\Omega\Omega^*)_{p,q} = 1$ and if $p \neq q$, $e^{i\frac{\pi}{n}(p-q)} \neq 1$ and:

$$\sum_{j=1}^{2n} [e^{i\frac{\pi}{n}(p-q)}]^{(j-1)} = \frac{1 - e^{2i(p-q)\pi}}{1 - e^{i\frac{\pi}{n}(p-q)}} = 0$$

and then $(\Omega\Omega^*)_{p,q} = 0$. Therefore $\Omega^{-1} = \Omega^*$. Finally :

$$\Pi = \Omega\Delta\Omega^*$$

Define now :

$$A := \Omega\, diag\left(\left(\sqrt{\sum_{j=0}^{2n-1} \gamma_{j+1}\omega_n^{jk}}\right)_{k=0,\dots,2n-1}\right)\Omega^*$$

so that we have the decomposition :

$$\Pi = AA^T$$

Now that we have established such a decomposition, the key point is that if we multiply a vector $x \in \mathbb{R}^{2n}$ with matrix Ω, we are applying a discrete Fourier transform to vector x. Indeed:

$$(\Omega x)_k = \frac{1}{\sqrt{2n}}\sum_{j=0}^{2n-1} x_j\omega_n^{jk} = \frac{1}{\sqrt{2n}}\sum_{j=0}^{2n-1} x_j e^{-2i\pi\frac{jk}{2n}} = \frac{1}{\sqrt{2n}} DFT(x)_k$$

Analogously the multiplication with Ω^* corresponds to an inverse discrete Fourier transform :

$$(\Omega^* x)_k = \frac{1}{\sqrt{2n}}\sum_{j=0}^{2n-1} x_j\bar{\omega_n}^{jk} = \frac{1}{\sqrt{2n}}\sum_{j=0}^{2n-1} x_j e^{2i\pi\frac{jk}{2n}} = \sqrt{2n}\, IDFT(x)_k$$

The advantage is that these multiplications can be algorithmically computed using the *fast Fourier transform* (fft) which would cost $O(n \log n)$ instead of $O(n^2)$ for a standard evaluation of $Q * x$.

Therefore, we can now formulate the efficient algorithm to simulate the Gaussian process on the time grid $\{t_0 + k\Delta \mid k = 0, \dots, n\}$ given that associated matrix Π is positive semi-definite.

Algorithm 3 Simulate efficiently a Gaussian process

Require: Mean $\mu \in \mathbb{R}$ and covariance function C of a stationary Gaussian process, $\{t_0, \dots, t_n\}$ a regular time grid, m the number of samples
Define $\gamma = (c_0, c_1, \dots, c_{n-1}, c_n, c_{n-1}, \dots, c_2, c_1)$ with $c_k := C(t_0, t_k)$
Compute $\lambda = DFT(\gamma)$ and verify that $\lambda_k \geq 0$ for all $k = 0, \dots, 2n-1$.
for $i = 1$ up to m **do**
Simulate 2n independant samples from the standard normal distribution $\mathbf{Z} = (Z_0, \dots, Z_{2n-1})$
Compute $\hat{\mathbf{X}} = DFT\Big(diag(\sqrt{\lambda_0}, \dots, \sqrt{\lambda_{2n-1}}) IDFT(\mathbf{Z})\Big)$
Save the new sample path $\mu + \hat{\mathbf{X}}_{0:n}$
end for

The total complexity of generating m simulated Gaussian vectors is $O(m \times (n \log n))$.

3.3 Simulation of fractional Brownian motion

Thanks to self-similarity of fractional Brownian motion, it is sufficient to simulate the process the unit time grid $\{0, 1, \dots, n\}$ and then rescale the resulting paths by Δ^H. We want to use the previous efficient algorithm. However, the fractional Brownian motion is not itself stationary. In order to tackle this, consider the increment process $\delta X := (B^H_{t+1} - B^H_t)_{t \geq 0}$. It has the covariance structure:

$$\begin{aligned}
\mathbb{E}(\delta X_t \delta X_s) &= \mathbb{E}\Big((B^H_{t+1} - B^H_t)(B^H_{s+1} - B^H_s)\Big) \\
&= \frac{V_H}{2}\Big[(|s+1|^{2H} + |t+1|^{2H} - |s-t|^{2H}) + (|s|^{2H} + |t|^{2H} - |s-t|^{2H}) \\
&- (|s+1|^{2H} + |t|^{2H} - |s+1-t|^{2H}) - (|s|^{2H} + |t+1|^{2H} - |s-t-1|^{2H})\Big] \\
&= \frac{V_H}{2}\Big[|(s-t)+1|^{2H} + |1-(s-t)|^{2H} - 2|s-t|^{2H}\Big]
\end{aligned}$$

which yields that δX is stationary. Actually, we already proved (theorem 2) that fractional Brownian motion has stationary increments. Now let $\Delta > 0$ and define the mean zero Gaussian vector $\tilde{X}$ by:

$$\begin{aligned}
\tilde{X}_k &:= \Delta^H \sum_{j=1}^{k} \delta X_{j-1} \qquad k = 0, \dots, n \\
&= \Delta^H (B^H_k - B^H_0) = \Delta^H B^H_k
\end{aligned}$$

From this definition, one has :

$$\mathbb{E}(\tilde{X}_j \tilde{X}_k) = \Delta^{2H} \mathbb{E}(B^H_k B^H_j) = \Delta^{2H} R_H(k, j) = R_H(\Delta k, \Delta j)$$

Therefore, $\tilde{X}$ represents an evaluation of a fractional Brownian motion on the time grid $\{0, \Delta, 2\Delta, \ldots, n\Delta\}$.

It can be shown that the covariance matrix of the increment process δX can always be embedded into a positive definite circulant matrix as described in the previous section. It garantees that one can always apply the efficient Algorithm 3 to simulate the increments of a fractional Brownian motion. Thus, we have the following algorithm.

Algorithm 4 Simulate fractional Brownian motion

Require: H the Hurst parameter, n the size of the time grid, Δ the mesh of the time grid, m the number of samples

Define $c = \left(\frac{1}{2}(|k+1|^{2H} + |k-1|^{2H}) - |k|^{2H} \right)_{0 \leq k \leq n-1}$.

Use Algorithm 3 with c to simulate $(\delta X^{(k)})_{1 \leq k \leq m}$ where each $\delta X^{(k)}$ is a sample of the increment process on $\{0, \Delta, 2\Delta, \ldots, (n-1)\Delta\}$.

for $i = 1$ up to m **do**

Save the new sample $\mathbf{X}^{(k)} := \left(\Delta^H \sum_{l=1}^{j} \delta X_{l-1}^{(k)} \right)_{0 \leq j \leq n}$.

end for

Return $(\mathbf{X}^{(k)})_{1 \leq k \leq m}$.

Thanks to the *fast Fourier transform* (fft) which costs $O(n \log n)$, simulation a m sample-paths of fractional Brownian motion using the efficient simulation algorithm costs $O(m \times (n \log(n)) \times n)$. This is the algorithm we will use to generate fractional Brownian motion sample-paths as well as fractional Ornstein-Uhlenbeck sample-paths in the next section.

4 Finance : Rough Fractional Stochastic Volatility [10]

In the article *Volatility is Rough* [10], authors seek to model the volatility process with high frequency data. More precisely, the idea is to model log-volatility as a fractional Ornstein-Uhlenbeck process.

4.1 Literature Review

In 1998, Comte and Renault [1] proposed to model log-volatility using fractional Brownian motion $(B_t^H)_{t\geq 0}$ with a Hurst parameter $H > 1/2$. The objective of choosing $H > 1/2$ was to model volatility persistence, a widely accepted stylized fact. The model is called the Fractional Stochastic Volatility model (FSV). Remind that Hurst parameter is of course a smoothness parameter of the process in the sense that :

$$\mathbb{E}(|B_{t+\Delta}^H - B_t^H|^q) = K_q \Delta^{qH} \qquad (\star)$$

and as we have seen in the first section, this process exhibits long memory increments when $H > 1/2$ since :

$$\sum_{n=0}^{+\infty} Cov(B_1^H, B_{n+1}^H - B_n^H) = +\infty$$

Therefore, the FSV model produces trajectories with the long memory stylized fact.

In the article *Volatility is Rough* [10], authors chose to model high-frequency log-volatility data just like the FSV model but with a Hurst parameter $H < 1/2$ and called it Rough Fractional Stochastic Volatility model (RFSV). More precisely, the idea is to model log-volatility as a fractional Ornstein-Uhlenbeck process with a Hurst parameter $H < 1/2$. What is worth noting is that, even with a Hurst parameter which suggests low persistence, data generated from this model satisfies long memory.

In fact, the authors suggest that volatility features roughness, and the roughness property of volatility in financial markets may arise from two phenomena. The first phenomenon is the high degree of endogeneity present in financial markets, where electronic high-frequency traders react algorithmically to the orders of other participants. The second phenomenon is the long-term impact of a given order on the following ones. This effect is likely due to the practice of splitting a large order (known as a parent order) into smaller orders (known as child orders) that are executed over an extended period. The purpose of this approach is to mitigate price deterioration. Ultimately, the combination of these two phenomena leads to a superposition effect that generates the irregular volatility observed in the markets.

There is another issue with classical stochastic volatility models such as the Hull and White [9], Heston [8], and SABR [13] : they do not fit the volatility surface. Indeed, an important stylized fact of traditional Equity volatility surface (SP500 for instance) is that the at-the-money volatility skew as a function of expiry, $\Psi(\tau) := \left| \frac{\partial}{\partial k} \sigma_{BS}(k, \tau) \right|_{k=0}$, fits a power-law of the form $\Psi(\tau) = A\tau^{-\alpha}$, $\alpha > 0$. The problem is that these stochastic volatility models generate a term-structure of ATM skew that is constant when τ is close to zero. Fukasawa [5] proved that a stochastic volatility model where volatility process is driven by a fractional Brownian motion has an ATM skew of the form $\Psi(\tau) = \tau^{H-1/2}$ for small τ.

4.2 Methodology

4.2.1 The model

The main idea of the article was to model log-volatility with a fractional Brownian motion, that is a model of the type :

$$\log \sigma_{t+\Delta} - \log \sigma_t = \nu(B^H_{t+\Delta} - B^H_t) \qquad (\star\star)$$

This model is not stationary, which is a desirable property. Thus, the considered model for the log-volatility is the fractional Ornstein-Uhlenbeck (fOU) model with a very long reversion time scale. It is the stationary solution of the stochastic differential equation :

$$\textbf{(fOU)} \qquad dX_t = \nu dB^H_t - \alpha(X_t - m)dt, \qquad t \in \mathbb{R}$$

We have seen in **2.4 fractional Ornstein-Uhlenbeck** that the explicit form of the solution is given by :

$$X_t = \int_{-\infty}^{t} e^{-\alpha(t-s)} dB^H_s + m$$

and finally, the RFSV model is :

$$\sigma_t = e^{X_t}$$

where X_t satisfies **(fOU)** with $\nu > 0$, $\alpha > 0$, $m \in \mathbb{R}$ and $H < 1/2$. The advantage of this model is that it is stationnary and setting α very close to zero, log-volatility behaves like fractional Brownian motion which is what we aimed at. Indeed, setting $\alpha = 0$ yields $(\star\star)$ and the following theorem specify how close the solution of the SDE and the fractional Brownian motion are :

Theorem 16. *Let B^H be a fractional Brownian motion and X^α defined in (**fOU**) for a given $\alpha > 0$. Then,*

$$\mathbb{E}(\sup_{t\in[0,T]} |X^\alpha_t - X^\alpha_0 - \nu B^H_t|) \xrightarrow[\alpha\to 0]{} 0$$

There is the corollary :

Theorem 17. *Let $q > 0$, $t > 0$, $\Delta > 0$. We have :*

$$\mathbb{E}[|X^\alpha_{t+\Delta} - X^\alpha_t|^q] \xrightarrow[\alpha\to 0]{} \nu^q K_q \Delta^{qH}$$

It justifies that when choosing α close to zero, using the solution of (**fOU**) to model log-volatility remains consistent with empirical observations and justifies the choice of the RFSV model for modeling our volatility high-frequency data time series.

4.2.2 The methodology

The methodology involves initially questioning the applicability of the model proposed in the article *Volatility is Rough* [10] in terms of its suitability for fitting the data. Specifically, it aims to determine whether modeling the volatility time series using fractional Brownian motion is appropriate.

This entails first examining the data over a specific sample period as well as specific asset to assess whether log-volatility exhibits Gaussian increments and satisfies the relationship:

$$\mathbb{E}(|X_{t+\Delta} - X_t|^q) = K_q \Delta^{qH} \qquad (\star)$$

Next, if the model proves to be a good fit, we examine whether the term structure of the volatility surface exhibits the desired shape. That is we need to prove that the term-structure of ATM skew fits a power-law of the form $\Psi(\tau) = A\tau^{-\alpha}$, $\alpha > 0$, and because Fukasawa [5] proved that a stochastic volatility model where volatility process is driven by a fractional Brownian motion has an ATM skew of the form $\Psi(\tau) = \tau^{H-1/2}$ for small τ, we only need to show that the estimated smoothness parameter H in model specification is lower than 1/2.

The last step of the methodology is to generate and plot trajectories of the specified model to compare their graphs with the volatility time series.

The article *Volatility is Rough* [10] analyzes the period from 01/03/2000 to 03/31/2014. However, in the next section, we will present daily data obtained from a longer period, starting from 01/03/2000 and extending until 12/05/2017. Initially, we replicate the results of the article by conducting the analysis on the same period as mentioned earlier, referring to it as the Referring Period. Subsequently, we perform the estimation across different indexes within this Referring Period. In the third section, we challenge the model and estimate the smoothness parameter during the Great Financial Crisis to see how log-volatility behaves over a shorter period and to compare the regularity of the volatility process. This period is referred to as the Stress Period, spanning from 06/29/2007 to 12/31/2010. Finally, we apply the methodology to the Out-of-the-Sample Period, which ranges from 04/01/2014 to 12/05/2017 to test its robustness.

4.3 Data

We obtained data from the Oxford-Man Institute, a world-leading research center in quantitative finance, since data collection has been a true issue due to the unavailability of high-frequency data from standard market data providers for free.

The data sample consists of daily non-parametric estimates of volatility for 20 financial indexes, including realized variance (rv) and realized kernel (rk) estimates, obtained from the Oxford-Man Institute's Realized Library. The formulas for realized variance and realized kernel are detailed in [6]. It is worth noting that, unlike realized variance, realized kernel estimates the appropriate volatility quantity even when the returns are contaminated with noise. Thus, we will work with realized kernel estimates.

Here are the descriptive statistics as well as the time series of the SP500 realized volatility over the Referring Period (01/03/2000 to 03/31/2014).

Table 1: Descriptive statistics of the SP500 realized kernel (rk) over the Referring Period (01/03/2000 to 03/31/2014)

Count	3553
mean	0.9374%
std	0.6153%
min	0.1533%
0.25 quantile	0.5549%
0.5 quantile	0.7871%
0.75 quantile	1.1001%
max	9.6503%

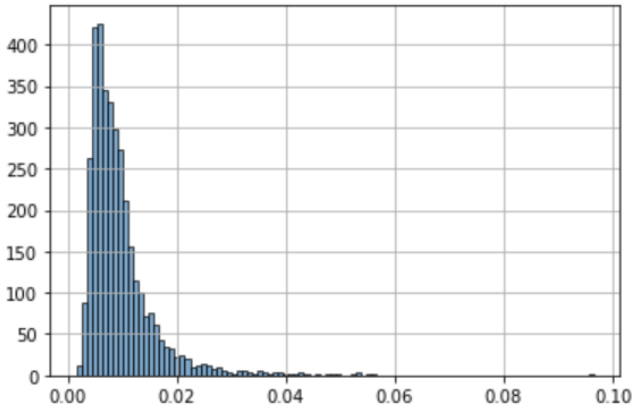

Figure 2: Volatility distribution of the SP500 (Referring Period)

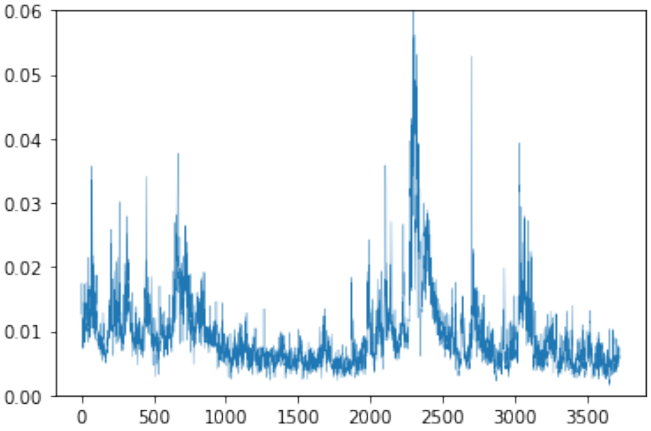

Figure 3: Volatility time series of the SP500 over the Referring period

4.4 Analysis and Results

4.4.1 Referring period

Let's define :

$$m(q, \Delta) := \frac{1}{N} \sum_{k=1}^{N} |\log(\sigma_{k\Delta}) - \log(\sigma_{(k-1)\Delta})|^q$$

If we assume $(\log(\sigma_t))_{t \geq 0}$ has stationary increments, according to the law of large number, $m(q, \Delta)$ is the empirical counterpart of :

$$\mathbb{E}[|\log(\sigma_\Delta) - \log(\sigma_0)|^q]$$

Of course, note that we are using a proxy (rv or rk) for the true spot market volatility. Let's regress now log $m(q, \Delta)$ against $\log \Delta$ for the SP500 index for the lag Δ varying from 1 to 100. It is important to note that the higher the lag, the fewer the members in the sum and the less precise the convergence of $m(q, \Delta)$ towards the expectation.

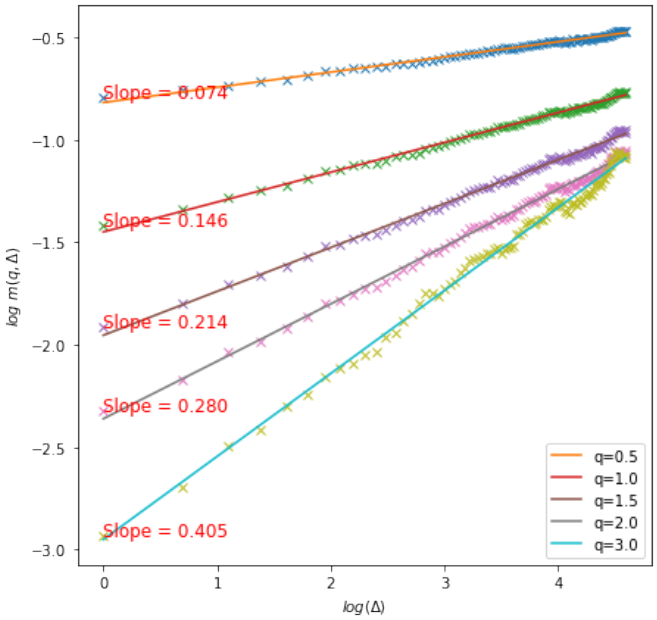

Figure 4: $\log m(q, \Delta)$ as a function of $\log \Delta$, SP500, period : 01/03/2000-03/31/2014

For the first regression line ($q = 0.5$), the result of the regression model appears to be an excellent fit to the data, with a high R-squared value of 0.992. The estimated coefficients are statistically significant, with very low p-values (close to zero). The p-value associated with the F-statistic is extremely low (1.39e-104), indicating that the overall model is significant. The Durbin-Watson statistic is 0.562, indicating positive autocorrelation of the residuals. To conclude, it appears a consistent linear realtionship between $\log m(q, \Delta)$ and $\log \Delta$, which means the following relationship is verified :

$$\mathbb{E}[|\log(\sigma_\Delta) - \log(\sigma_0)|^q] = K_q \Delta^{\zeta_q}$$

This expression is close to $(\star)$ and in that sense, it is coherent to consider a fractional Brownian motion to model log-volatility. In $(\star)$, we had $\zeta_q = qH$. Let's plot ζ_q against q to compare its shape with $q \to qH$.

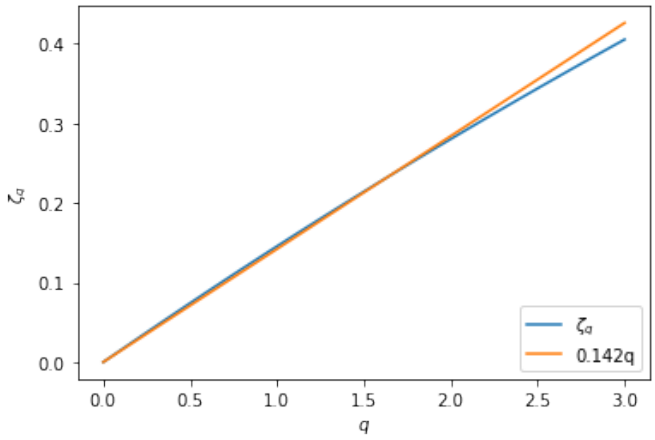

Figure 5: ζ_q as a function of q, SP500, period : 01/03/2000-03/31/2014

We remark that the curve is slightly concave which relates finite sample size and is thus not significant. Therefore, we can consider the slope of the curve to be a smoothness coefficient : we can consider $\zeta_q = 0.142 \times q$, 0.142 being the smoothness coefficient.

Another important requirement for the log-volatility to being modeled by fBm is to have gaussian increments. This all the more important given that the distribution of increments of log-volatility to be close to Gaussian is a well-established stylized fact. We can see on the following graphs (Figure 6) that, whatever the lag is, the distribution of increments of log-volatility data fits a gaussian distribution.

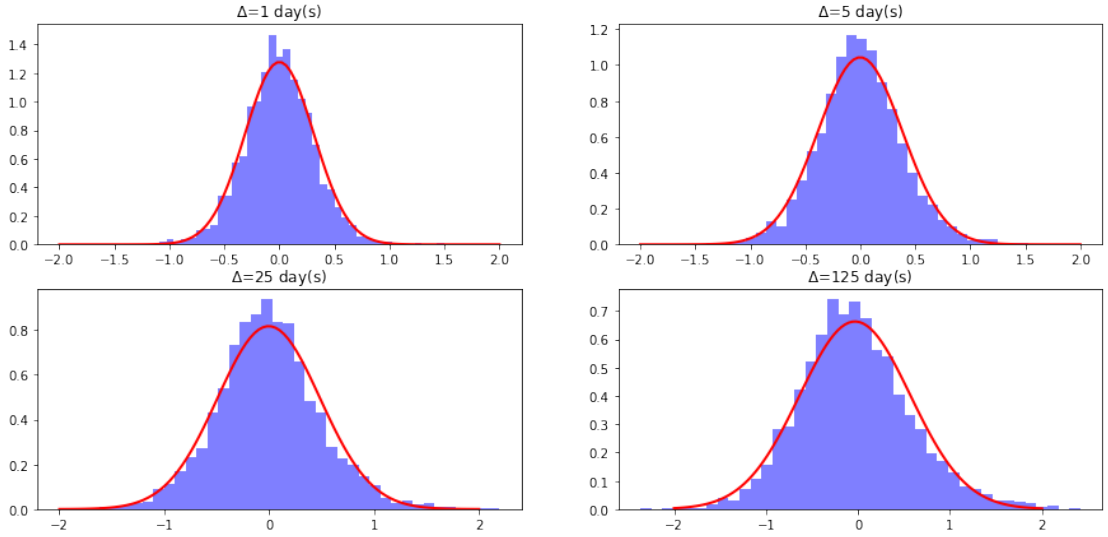

Figure 6: Histograms of the SP500 log-volatility increments $\log \sigma_{t+\Delta} - \log \sigma_t$ for different lags Δ; normal fits in red

The second step of the methodology is that we have found a coefficient of 0.142 which is lower than 0.5. We have seen in a previous remark that if we want to model volatility through fractional Brownian motion paths, the model ATM volatility skew as a function of maturity behaves as $\Psi(\tau) = \tau^{H-1/2}$ when τ is small. Therefore, choosing a smoothness coefficient H lower than $1/2$ is a crucial requirement for $\Psi(\tau) = \tau^{H-1/2}$ to explode when $\tau \to 0$ and then for the chosen model to fit the term-structure of the market ATM volatility skew. We will see various values of smoothness empirical estimations for different indexes in the subsection **4.4.2 Across indexes**.

Let's see now how the model performs in generating volatility time series, it constitutes the third step of the methodology. We want to compare the simulated volatility with the the realized volatility of the SP500 for the same reference period. Let's simulate now the trajectory of the specified model. Over T=3500 days, we need to choose $\alpha << 1/T$, choose $\alpha = 5 \times 10^{-4}$. The other chosen parameters are : $H = 0.14$, $m = X_0 = -5$, $\nu = 0.3$. Here are two simulated trajectories of the corresponding fractional Ornstein-Uhlenbeck.

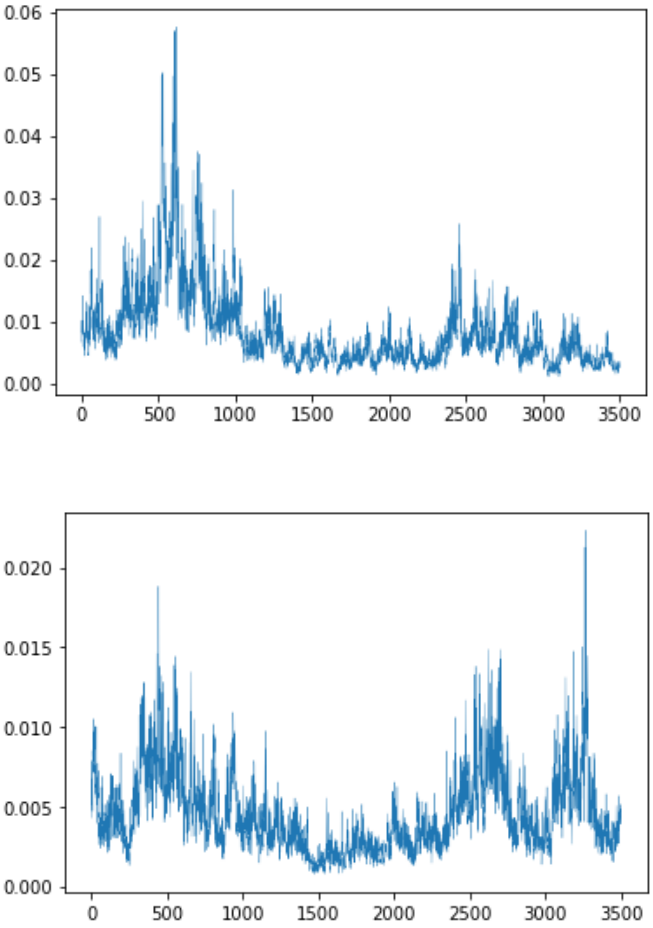

Figure 7: Simulated paths of specified RFSV model

The model seems to have the same type of trajectories as the volatility time series. We can notice that in both graphs persistent periods of high volatility alternate with low volatility periods. Thus the model simulate rather accurately the long-memory volatility stylized fact.

We can also show the scaling property of $m(q, \Delta)$:

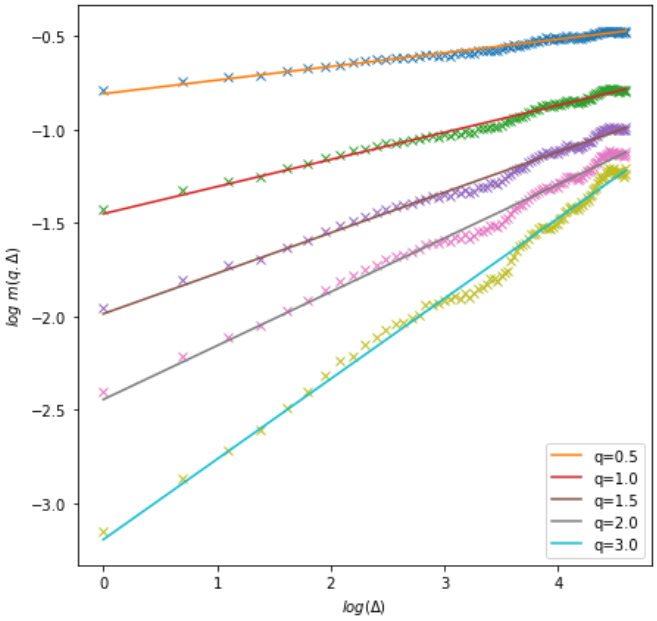

Figure 8: $\log(m(q,\Delta))$ as a function of $\log(\Delta)$, simulated data

4.4.2 Across indexes

Since data is available for several indexes, we performed the smoothness estimation for each index log-volatility. The results are based on the realized kernel and are given in the table below.

Table 2: Estimation of ζ_q for several indexes of the Oxford-Man dataset

index	$\zeta_{0.5}/0.5$	$\zeta_1/1$	$\zeta_{1.5}/1.5$	$\zeta_2/2$	$\zeta_3/3$
SPX2	0.136	0.133	0.131	0.128	0.123
FTSE2	0.153	0.149	0.144	0.139	0.127
N2252	0.120	0.118	0.115	0.113	0.106
GDAXI2	0.175	0.168	0.161	0.153	0.140
RUT2	0.126	0.122	0.118	0.114	0.108
AORD2	0.089	0.087	0.085	0.082	0.077
DJI2	0.129	0.126	0.123	0.120	0.114
FCHI2	0.160	0.155	0.150	0.144	0.134
HSI2	0.099	0.099	0.099	0.100	0.101
KS11	0.132	0.130	0.128	0.126	0.120
AEX	0.171	0.167	0.162	0.156	0.145
SSMI	0.179	0.179	0.178	0.176	0.169
IBEX2	0.149	0.144	0.139	0.134	0.124
NSEI	0.110	0.107	0.105	0.101	0.092
MXX	0.090	0.088	0.086	0.083	0.078
BVSP	0.111	0.109	0.107	0.105	0.101
STOXX50E	0.158	0.150	0.141	0.130	0.100
FTSTI	0.123	0.124	0.124	0.123	0.119

We observe a slight convexity in the ζ curve, which is considered negligible. Additionally, it is evident that the roughness parameters across all financial indexes are very close to each other. Thus, roughness appears to be a universal characteristic of the realized measures of volatility logarithm in equity indexes. Notably, a recent study by Bennedsen et al. [11] conducted in 2021 examined 10,744 individual equities across ten industry sectors from January 2, 2003, to December 31, 2013. Their findings indicate significant roughness and, more importantly, no systematic differences in roughness estimates across sectors. In summary, the study demonstrates that roughness and persistence of log volatility extend to the to the individual equity level.

4.4.3 Stress period

Hence, an interesting starting point for further analysis would be to assess the model's consistency and to estimate smoothness during stress periods, such as the Great Financial Crisis. Specifically, examining the period from mid-2007 to the end of 2010, we obtained the following descriptive statistics :

Table 3: Descriptive statistics of the SP500 realized kernel (rk) over the Stress period

Count	878
mean	1.2631%
std	0.8796%
min	0.2199%
0.25 quantile	0.7452%
0.5 quantile	1.0113%
0.75 quantile	1.4626%
max	9.6503%

The mean is logically significantly higher and we can notice that the maximum over the whole available period is reached in this Stress period. The regression of $\log(m(q, \Delta))$ against $\log(\Delta)$ is performed with less values of lag Δ because there is only 878 available data against 3553 previously and, as explained before, we must limit the length of the lag so that the empirical mean remains close to the expectation.

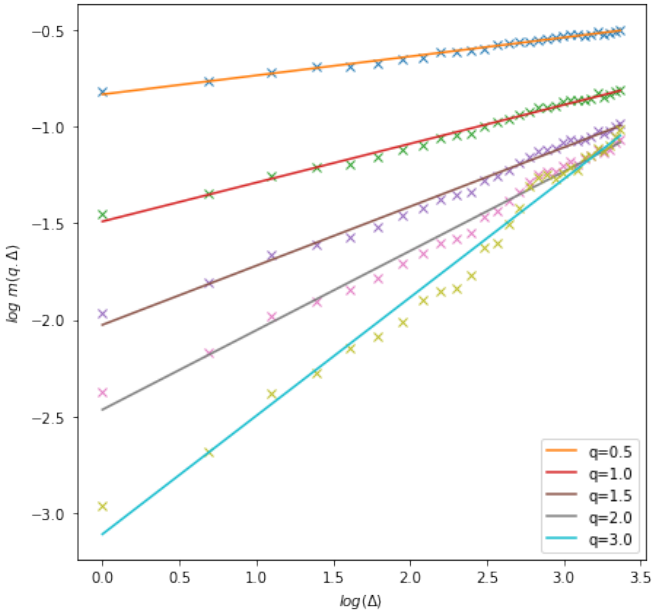

Figure 9: $\log m(q, \Delta)$ as a function of $\log \Delta$, SP500, period : 06/29/2007-12/31/2010

We can observe that the linear relationship holds. Let's examine the results of the last regression line ($q = 3$). R-squared value of 0.983 proves a strong fit. Both the intercept and the coefficient associated with the independent variable are statistically significant, with very low p-values. The Durbin-Watson statistic is 0.508, suggesting a moderate level of positive autocorrelation in the residuals. The F-statistic's p-value is extremely low (2.18e-25), indicating that the overall model is highly statistically significant. The Jarque-Bera test is not significant (p-value of 0.958), proving that the residuals do not exhibit significant skewness or kurtosis. The Omnibus test demonstrates no significance (p-value of 0.983), indicating that the residuals do not deviate too significantly from normality.

Let us plot now the smoothness ζ_q to compare the smoothness coefficient.

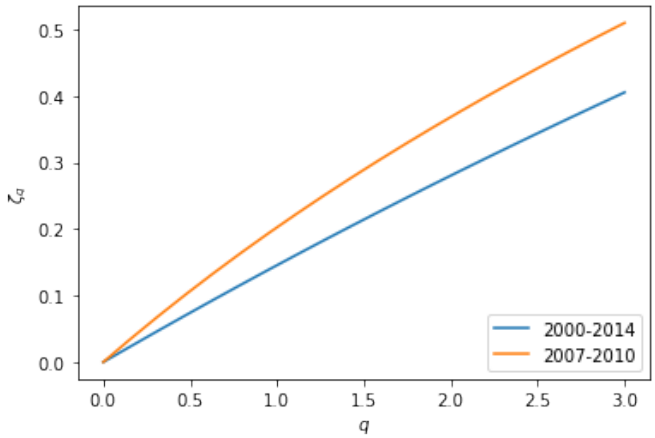

Figure 10: ζ_q as a function of q, SP500, period : 06/29/2007-12/31/2010

We can note that during the crisis, the smoothness parameter is higher. It seems to indicate that volatility exhibits less roughness during periods of market turmoil, possibly due to more sustained trading activity during such times. However, we cannot draw any conclusion from a single time series. In the article [11], the authors analyzed E-mini SP500 transcation data from January 3, 2005 until December 31, 2014 to plot the rolling-window index roughness estimation as a function of time. The window length is 900 observations, corresponding to roughly 150 days.

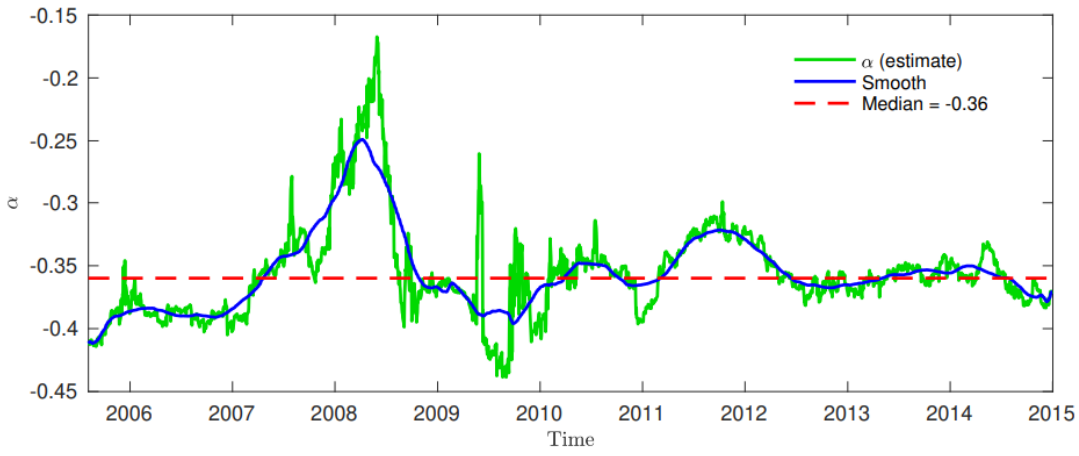

Figure 11: Graph from [11], rolling-window NLLS estimates of roughness

What is interesting to notice is the consistently high smoothness estimates throughout the crisis, which is in tune with our previous single estimation.

4.4.4 Out-of-the-sample period

Let's proceed with the model on the period spanning from 04/01/2014 to 12/05/2017.

Table 4: Descriptive statistics of the SP500 realized kernel (rk) over the Out-of-the-Sample Period

Count	929
mean	0.5273%
std	0.3158%
min	0.1186%
0.25 quantile	0.3302%
0.5 quantile	0.4536%
0.75 quantile	0.6201%
max	4.4624%

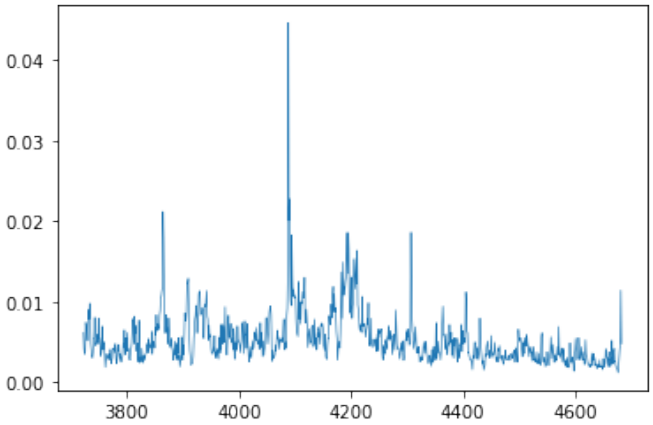

Figure 12: Volatility time series of the SP500 over the Out-of-the-sample period

As usual, let's regress $\log(m(q, \Delta))$ against $\log(\Delta)$.

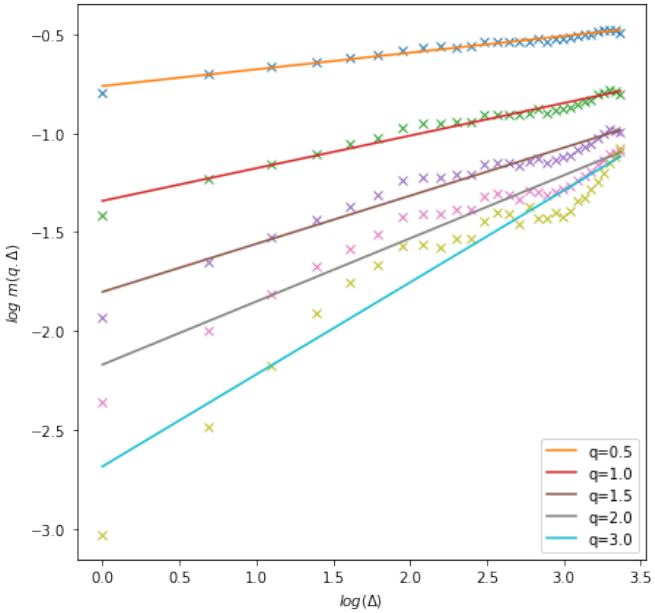

Figure 13: $\log m(q, \Delta)$ as a function of $\log \Delta$, SP500, Out-of-the-sample period

The relationship seems to be less robust than before, especially for higher values of q. Let's examine the regression for ($q = 3$). The model finally provides a good fit, with an R-squared value of 0.915. The coefficient is significant, with a very low p-values. As before, the p-value associated with the F-statistic is extremely low (5.78e-16). The Omnibus test shows no significance (p-value of 0.287), indicating that the residuals do not deviate significantly from normality.

Finally, even though when the value of q increases, the model loses in robustness, the model is rather accurate for this period.

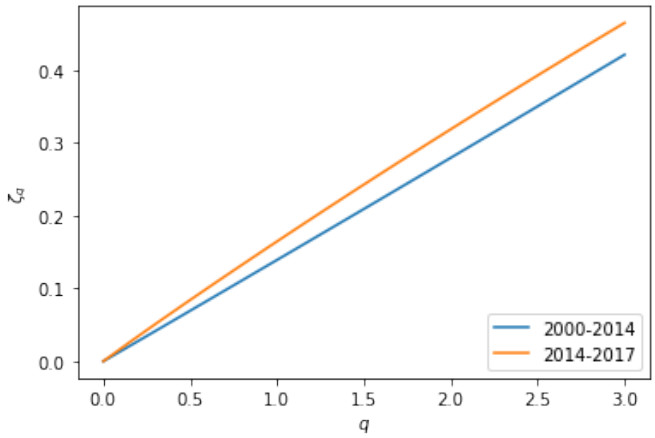

Figure 14: ζ_q as a function of q, SP500, Out-of-the-sample period

We can notice that the smoothness of the Out-of-the-sample period is slightly higher than the smoothness of the Referring period, the smoothness parameter being 0.164, compared to 0.142.

4.4.5 Conclusion

The model exhibits an excellent fit to the data, consistently estimating rough parameters, which are lower than 1/2. This alignment is significant because Fukasawa [5] demonstrated that a stochastic volatility model, in which the volatility process is driven by a fractional Brownian motion, results in an ATM skew of the form $\Psi(\tau) = \tau^{H-1/2}$ for small τ. Thus, the model captures the appropriate shape of the term structure. Furthermore, we have observed that volatility displays smooth trajectories during stress periods, such as the Great Financial Crisis. Lastly, we have also observed that roughness appears to be a universal characteristic of the realized measures of log-volatility in equity indexes.

The main drawback of this analysis lies in the data collection process. Due to limited access to high-frequency data, we have relied on the data used in the article *Volatility is Rough* [10], with approximately three years of additional daily data. By conducting the analysis on a period that was not examined in the original article, we demonstrate the robustness of the model. However, it would have been even more advantageous to test the model on more recent data, such as during the Covid-19 crisis, in order to evaluate and estimate the roughness, or to apply the model to individual equities or across different equity parameters, such as capitalization or sector.

Conclusion

We have established a definition for the integral with respect to fractional Brownian motion and investigated Rough Path theory. We have been able to define fractional Ornstein-Uhlenbeck processes and derive their explicit form. By using efficient simulation techniques for Gaussian processes, we have developed an algorithm that can simulate fractional Brownian motion and subsequently simulate fractional Ornstein-Uhlenbeck processes. This puts us in a favorable position to fully grasp the purpose of the RFSV model. By testing the model over different subperiods and estimating roughness parameter of the data, we have concluded that the RFSV model exhibits an excellent fit to the data of severeal indexes and that the model captures the appropriate shape of the ATM skew. The main inconvenient of the methodology is the lack of variety in the high-frequency data sources.

Some possible future research topics could include exploring deeper the Rough Path theory and being able to apprehend rough differential equations, or providing a mathematical justification for the observed irregularity of volatility in microstructure models (such as modeling order flow through Hawkes processes, for instance [16]).

A Additional Proofs

Theorem 3 : Hölder continuity

Proof. For any $(s,t) \in \mathbb{R}, B_t^H - B_s^H$ is a gaussian random variable of mean 0 and of variance:

$$\begin{aligned}\mathbb{E}((B_t^H - B_s^H)^2) &= \mathbb{E}((B_t^H)^2) + \mathbb{E}((B_s^H)^2) - 2\mathbb{E}(B_t^H B_s^H) \\ &= V_H t^{2H} + V_H s^{2H} - V_H(t^{2H} + s^{2H} - |s-t|^{2H}) \\ &= V_H |t-s|^{2H}\end{aligned}$$

Hence we have:

$$\forall a > 0, (s,t) \in \mathbb{R}^2, \mathbb{E}((B_t^H - B_s^H)^a) = \underbrace{V_H^{a/2}\mathbb{E}(|N|^a)}_{C_a^H} |t-s|^{aH}$$

where $N \sim \mathcal{N}(0,1)$. Moreover, $C_a^H < \infty$ since $N \in L^p(\mathbb{P}), \forall p < \infty$. Then the Kolmogorov continuity theorem garanties the existence of a γ-Hölder continuous version $\tilde{B}^H$ of B^H of any $\gamma \in]0, H[$. Hölder continuity implies continuity, hence $\tilde{B}^H$ and B^H are indiscernable, that is $\mathbb{P}(\underbrace{\{\omega \in \Omega : \forall t \in \mathbb{R}, \tilde{B}_t^H(\omega) = B_t^H(\omega)\}}_{\text{may not be measurable...}}) = 1$ or $\exists N \subset \Omega$ negligible, $\forall \omega \notin N, \forall t \in \mathbb{R}, \tilde{B}_t^H(\omega) = B_t^H(\omega)$. Hence, sample-paths of $(B_t^H)_{t\in\mathbb{R}}$ are almost-surely Hölder continuous of any order $\gamma < H$. □

Theorem 4 : existence and unicity of fractional Brownian motion.

Proof. ([12]) From previous remark, there is only to prove that $R_H : \mathbb{R}^2 \to \mathbb{R}$ is symmetrical which is immediate, and positive semi-definite. Let's show that if $m \in \mathbb{N}$:

$$\forall s = (s_1, \ldots, s_m),\ u = (u_1, \ldots, u_m) \in \mathbb{R}^m\ :\quad \sum_{i=1}^m \sum_{j=1}^m R_H(s_i, s_j) u_i u_j \geq 0$$

First, one has :

$$|x|^{2H} = \frac{1}{c_H} \int_0^\infty \frac{1 - e^{-u^2 x^2}}{u^{1+2H}} du$$

where $c_H := \int_0^\infty \frac{1-e^{-u^2}}{u^{1+2H}} du < \infty$. Indeed, performing a change of variable $v = |x|u$, one has :

$$\int_0^\infty \frac{1 - e^{-u^2x^2}}{u^{1+2H}} du = \int_0^\infty \frac{1 - e^{-v^2}}{v^{1+2H}} |x|^{1+2H} \frac{dv}{|x|} = |x|^{2H} \left(\int_0^\infty \frac{1 - e^{-v^2}}{v^{1+2H}} dv \right) = c_H |x|^{2H}$$

Therefore, for any non negative s, t, one has :

$$\begin{aligned}&\frac{V_H}{2}(|t|^{2H} + |s|^{2H} - |t-s|^{2H}) \\ &= \frac{V_H}{2c_H} \int_0^\infty \frac{(1 - e^{-u^2s^2})(1 - e^{-u^2t^2})}{u^{1+2H}} du + \frac{V_H}{2c_H} \int_0^\infty \frac{e^{-u^2s^2}(e^{2u^2st} - 1)e^{-u^2t^2}}{u^{1+2H}} du \\ &= \frac{V_H}{2c_H} \int_0^\infty \frac{(1 - e^{-u^2s^2})(1 - e^{-u^2t^2})}{u^{1+2H}} du + \frac{V_H}{2c_H} \int_0^\infty \frac{e^{-u^2s^2}[\sum_{n=1}^\infty \frac{(2u^2st)^n}{n!}]e^{-u^2t^2}}{u^{1+2H}} du \\ &= \frac{V_H}{2c_H} \int_0^\infty \frac{(1 - e^{-u^2s^2})(1 - e^{-u^2t^2})}{u^{1+2H}} du + \frac{V_H}{2c_H} \sum_{n=1}^\infty \frac{2^n}{n!} \int_0^\infty \frac{t^n e^{-u^2t^2} s^n e^{-u^2s^2}}{u^{1-2n+2H}} du\end{aligned}$$

Therefore:

$$\forall s=(s_1,\dots,s_m),\ u=(u_1,\dots,u_m)\in\mathbb{R}^m\ :\sum_{i=1}^{m}\sum_{j=1}^{m}[\frac{V_H}{2}(|s_i|^{2H}+|s_j|^{2H}-|s_i-s_j|^{2H})]u_iu_j$$

$$=\frac{V_H}{2c_H}\int_0^\infty\frac{\left(\sum_{i=1}^m(1-e^{-u^2s_i^2})u_i\right)^2}{u^{1+2H}}du+\frac{V_H}{2c_H}\sum_{n=1}^{\infty}\frac{2^n}{n!}\int_0^\infty\frac{\left(\sum_{i=1}^m s_i^ne^{-u^2s_i}u_i\right)^2}{u^{1-2n+2H}}du\geq 0$$

□

Theorem 5 : Caracterisation of the convergence of Riemann-Stieltjes sums.

Proof. Suppose $I=\int_a^b f(x)d\phi(x)$ exists as a Stieltjes integral and let $\epsilon>0$. One has $\frac{\epsilon}{2}>0$ and by hypothesis, there is a $\delta>0$ such that :

$$\forall\tau,\psi\ :\quad |\tau|<\delta\implies|S_\tau^\psi(f,\phi)-I|<\frac{\epsilon}{2}$$

Let τ,τ' two subdivisions with meshes lower than δ. Hence we have :

$$|S_\tau^\psi(f,\phi)-S_{\tau'}^\psi(f,\phi)|\leq|S_\tau^\psi(f,\phi)-I|+|I-S_{\tau'}^\psi(f,\phi)|<\frac{\epsilon}{2}+\frac{\epsilon}{2}=\epsilon$$

Let's now prove the reciprocal.
First, let's prove that the limit does not depend on the chosen sequence of subdivision with mesh that goes to zero. Let $(\tau^{(n)})_{n\in\mathbb{N}}$ and $(\tau'^{(n)})_{n\in\mathbb{N}}$ two sequence of subdivisions with meshes that are going to zero such that $(S^\psi_{\tau^{(n)}}(f,\phi))_{n\in\mathbb{N}}$ and $(S^\psi_{\tau'^{(n)}}(f,\phi))_{n\in\mathbb{N}}$ converges toward I and I' respectively. Let $\epsilon>0$. Pick a $\delta>0$ as in hypothesis. We know that :

$$\exists N\in\mathbb{N},\ \forall n\geq N,\ |\tau^{(n)}|,|\tau^{(n)}|<\delta$$

One obtains from hypothesis:

$$|I-I'|\leq|S^\psi_{\tau^{(n)}}(f,\phi)-I|+|S^\psi_{\tau'^{(n)}}(f,\phi)-I'|+|S^\psi_{\tau^{(n)}}(f,\phi)-S^\psi_{\tau'^{(n)}}(f,\phi)|<3\epsilon$$

that is $I=I'$.

From the following lemma and the fact that the limit does not depends on the chosen sequence of subdivision, we just need to prove that for any sequence $(\tau^{(n)})_{n\in\mathbb{N}}$ of subdivision with mesh that goes to 0, there is $I\in V$ such that $S^\psi_{\tau^{(n)}}(f,\phi)\xrightarrow[n\to\infty]{}I$. Since V is Banach space, it is sufficent to prove that $\forall(\tau^{(n)})_{n\in\mathbb{N}}$ with $|\tau^{(n)}|\xrightarrow[n\to\infty]{}0$, $(S^\psi_{\tau^{(n)}}(f,\phi))_{n\in\mathbb{N}}$ is a Cauchy sequence.
So let's choose a sequence $(\tau^{(n)})_{n\in\mathbb{N}}$ with mesh going to zero and prove that $(S^\psi_{\tau^{(n)}}(f,\phi))_{n\in\mathbb{N}}$ is a Cauchy sequence. From hypothesis, if we let $\epsilon>0$ we can choose a $\delta>0$ such that :

$$\forall\tau,\tau'\ :\quad|\tau|,|\tau'|<\delta\implies|S_\tau^\psi(f,\phi)-S_{\tau'}^\psi(f,\phi)|<\epsilon\qquad(\triangle)$$

One has :

$$\exists N\in\mathbb{N},\ \forall n\geq N:\ |\tau^{(n)}|<\delta$$

Let $(k,l)\in\mathbb{N}^2$. If ($k\geq N$ and $l\geq N$), then $|\tau^{(k)}|,|\tau^{(l)}|<\delta$ and from ($\triangle$):

$$|S^\psi_{\tau^{(k)}}(f,\phi)-S^\psi_{\tau^{(l)}}(f,\phi)|<\epsilon$$

□

lemma 1. *Suppose there exists $I \in V$ such that for any sequence $(\tau^{(n)})_{n\in\mathbb{N}}$ of subdivision with mesh that goes to 0, $S^{\psi}_{\tau^{(n)}}(f,\phi) \xrightarrow[n\to\infty]{} I$. Therefore, $\int_a^b f d\phi$ exists and equals I.*

Proof. Perform the proof by contraposition. Let $I \in V$ and pick $\epsilon > 0$ such that, by hypothesis :

$$\forall \delta > 0,\ \exists \tau \text{ a subdivision such that } |\tau| < \delta \text{ and } |S^{\psi}_{\tau}(f,\phi) - I| \geq \epsilon$$

Let $n \in \mathbb{N}^*$. From previous statement, there is a subdivision $\tau^{(n)}$ such that $|\tau^{(n)}| < \frac{1}{n}$ and $|S^{\psi}_{\tau^{(n)}}(f,\phi) - I| \geq \epsilon$. Next, choose a higher $n \in \mathbb{N}^*$ and iterate to build a sequence of subdivisions with mesh that goes to zero such that $|S^{\psi}_{\tau^{(n)}}(f,\phi) - I|$ is always greater than ϵ. □

Theorem 8 : convergence in norm $\mathbb{L}^2$ of $Var^{\tau}_{\frac{1}{H}}(B^H)$.

Proof. Note first that :

$$\mathbb{E}(Var^{\tau}_{\frac{1}{H}}(B^H)) = \sum_{j=0}^{r-1} V_H^{1/2H}\mathbb{E}(|N|^{\frac{1}{H}})|t_{j+1} - t_j|^{\frac{1}{H}\times H} = V_H^{1/2H}\mathbb{E}(|N|^{\frac{1}{H}})t$$

Hence we need to prove that

$$\|Var^{\tau}_{\frac{1}{H}}(B^H) - tV_H^{1/2H}\mathbb{E}(|N|^{\frac{1}{H}})\|_{\mathbb{L}^2} = \mathbb{V}(Var^{\tau}_{\frac{1}{H}}(B^H)) = \mathbb{E}(Var^{\tau}_{\frac{1}{H}}(B^H)^2) - t^2V_H^{1/H}\mathbb{E}(|N|^{\frac{1}{H}})^2$$

converges to zero as $|\tau| \to 0$, that is to prove that :

$$\mathbb{E}(Var^{\tau}_{\frac{1}{H}}(B^H)^2) \to t^2V_H^{1/H}\mathbb{E}(|N|^{\frac{1}{H}})^2$$

as mesh goes to zero. Now let (X,Y) be a pair of independant standard gaussian random variables. Let's denote $\Delta_i B^H := B_{t_{j+1}} - B_{t_j}$. We already know that $\Delta_i B^H \sim V_H^{\frac{1}{2}}|t_{i+1} - t_i|^H X$ and we have :

$$\Delta_j B^H \sim Z_{(i,j)} := \underbrace{\frac{\mathbb{E}(\Delta_i B^H \Delta_j B^H)}{V_H^{1/2}|t_{i+1} - t_i|^H}}_{\omega^1_{i,j}} X + \underbrace{\sqrt{\frac{V_H|t_{i+1} - t_i|^{2H}V_H|t_{j+1} - t_j|^{2H} - \mathbb{E}(\Delta_i B^H \Delta_j B^H)^2}{V_H|t_{i+1} - t_i|^{2H}}}}_{\omega^2_{i,j}} Y$$

Indeed, by independance, $Z_{(j,i)}$ is a centered gaussian random variable of variance:

$$\begin{aligned}\mathbb{V}(Z_{(j,i)}) &= \left[\frac{\mathbb{E}(\Delta_i B^H \Delta_j B^H)}{V_H^{1/2}|t_{i+1} - t_i|^H}\right]^2 \times 1 + \left[\sqrt{\frac{V_H|t_{i+1} - t_i|^{2H}V_H|t_{j+1} - t_j|^{2H} - \mathbb{E}(\Delta_i B^H \Delta_j B^H)^2}{V_H|t_{i+1} - t_i|^{2H}}}\right]^2 \times 1 + 0 \\ &= V_H|t_{j+1} - t_j|^{2H}\end{aligned}$$

Next,

$$\begin{aligned}
\mathbb{E}(Var^{\tau}_{\frac{1}{H}}(B^H)^2) &= \mathbb{E}[(\sum_{j=0}^{r-1}(\Delta_j B^H)^{\frac{1}{H}})^2] \\
&= \sum_{j=0}^{r-1}\sum_{i=0}^{r-1}\mathbb{E}[(\Delta_j B^H)^{\frac{1}{H}}(\Delta_i B^H)^{\frac{1}{H}}] \\
&= \sum_{j=0}^{r-1}\sum_{i=0}^{r-1}\int_{\mathbb{R}}\int_{\mathbb{R}}(\omega^1_{i,j}x+\omega^2_{i,j}y)^{\frac{1}{H}}(V_H^{1/2}|t_{i+1}-t_i|^H x)^{\frac{1}{H}}d\mathbb{P}_X\otimes\mathbb{P}_Y(x,y) \quad \text{(independance)} \\
&= \frac{1}{2\pi}\int_{\mathbb{R}}\int_{\mathbb{R}}e^{-\frac{(x^2+y^2)}{2}}\sum_{j=0}^{r-1}\sum_{i=0}^{r-1}[V_H^{1/2}|t_{j+1}-t_j|^H|d_{i,j}x+\sqrt{1-d^2_{i,j}}y|]^{\frac{1}{H}}(V_H^{1/2}|t_{i+1}-t_i|^H|x|)^{\frac{1}{H}}dx\,dy \\
&= \frac{1}{2\pi}\int_{\mathbb{R}}\int_{\mathbb{R}}e^{-\frac{(x^2+y^2)}{2}}\underbrace{\sum_{j=0}^{r-1}\sum_{i=0}^{r-1}V_H^{1/H}|t_{j+1}-t_j|\,|t_{i+1}-t_i|\,|d_{i,j}x+\sqrt{1-d^2_{i,j}}y|^{\frac{1}{H}}|x|^{\frac{1}{H}}\,dx\,dy}_{f^{\tau}_H(x,y)} \quad (1)
\end{aligned}$$

setting :

$$d_{i,j} := \frac{\omega^1_{i,j}}{V_H^{1/2}|t_{j+1}-t_j|^H} = \frac{\mathbb{E}(\Delta_i B^H\Delta_j B^H)}{V_H|t_{i+1}-t_i|^H|t_{j+1}-t_j|^H}$$

which is bounded by 1. Indeed, from Cauchy-Schwarz inequality:

$$\mathbb{E}(\Delta_i B^H\Delta_j B^H) \le \sqrt{\mathbb{E}((\Delta_i B^H)^2)}\sqrt{\mathbb{E}((\Delta_j B^H)^2)} = \sqrt{V_H|t_{i+1}-t_i|^{2H}}\sqrt{V_H|t_{j+1}-t_j|^{2H}}$$

Next, one has :

$$\begin{aligned}
\forall(x,y)\in\mathbb{R}^2,\quad |f^{\tau}_H(x,y)-t^2|y|^{1/H}|x|^{1/H}| &= ||x|^{1/H}V_H^{1/H}\sum_{i,j}|t_{j+1}-t_j|\,|t_{i+1}-t_i|\,[|d_{i,j}x+\sqrt{1-d^2_{i,j}}y|^{\frac{1}{H}}-|y|^{\frac{1}{H}}] \\
&\le \frac{2}{H}|x|^{1/H}[|x|^{1/H}+|y|^{1/H}]\sum_{i,j}|t_{j+1}-t_j|\,|t_{i+1}-t_i|\,|d_{i,j}| \quad (2)
\end{aligned}$$

Now let $\epsilon\in]0,1]$.
Case 1 : If the pair (i,j) is such that $|t_i-t_i|\ge 4\frac{|\tau|}{\epsilon}$, then $\frac{t_{i+1}-t_i}{|t_i-t_i|}$ and $\frac{t_{i+1}-t_i}{|t_i-t_i|}$ are both lower than $\frac{\epsilon}{4}$. Using the below technical lemma with $s=t_i$, $t=t_j$, $u=t_{i+1}-t_i$ and $v=t_{j+1}-t_j$, one has :

$$\begin{aligned}
|d_{i,j}| &= \left|\frac{\mathbb{E}(\Delta_i B^H\Delta_j B^H)}{V_H|t_{i+1}-t_i|^H|t_{j+1}-t_j|^H}\right| \\
&= H(1-2H)\left|\frac{(t_{i+1}-t_i)(t_{j+1}-t_j)}{|t_i-t_j|^2}\right|^{1-H}+R\left(\frac{t_{i+1}-t_i}{t_i-t_j},\frac{t_{j+1}-t_j}{t_i-t_j}\right) \\
&\le H(1-2H)\left|\frac{(t_{i+1}-t_i)(t_{j+1}-t_j)}{|t_i-t_j|^2}\right|^{1-H}+C^H\min\left(\frac{t_{j+1}-t_j}{t_i-t_j},\frac{t_{i+1}-t_i}{t_i-t_j}\right)^3\left|\frac{t_{j+1}-t_j}{t_i-t_j}\right|^{-H}\left|\frac{t_{i+1}-t_i}{t_i-t_j}\right|^{-H} \\
&\le \epsilon^{2-2H}\underbrace{\left[\frac{H(1-2H)+\frac{C^H}{4}}{4^{2-2H}}\right]}_{C_H}
\end{aligned}$$

and of course one has :

$$\sum_{(i,j):|t_i-t_j|\geq 4\frac{|\tau|}{\epsilon}} |t_{j+1}-t_j|\,|t_{i+1}-t_i| \leq \sum_{i,j} |t_{j+1}-t_j|\,|t_{i+1}-t_i| = t^2$$

Case 2 : consider (i,j) is such that $|t_i - t_i| < 4\frac{|\tau|}{\epsilon}$. One still has $d_{i,j}$ bounded by 1 and furthermore, using Fubini-Tonelli:

$$\sum_{(i,j):|t_i-t_j|<4\frac{|\tau|}{\epsilon}} |t_{j+1}-t_j|\,|t_{i+1}-t_i| \leq 16t\frac{|\tau|}{\epsilon}$$

Finally, choosing $|\tau| \leq \epsilon^2$ and combining case 1 and case 2, one has :

$$\begin{aligned}\sum_{i,j} |t_{j+1}-t_j|\,|t_{i+1}-t_i|\,|d_{i,j}| &= \sum_{(i,j):|t_i-t_j|\geq 4\frac{|\tau|}{\epsilon}} |t_{j+1}-t_j|\,|t_{i+1}-t_i|\,|d_{i,j}| + \sum_{(i,j):|t_i-t_j|<4\frac{|\tau|}{\epsilon}} |t_{j+1}-t_j|\,|t_{i+1}-t_i|\,|d_{i,j}| \\ &\leq C[\epsilon^{2-2H}t^2 + \epsilon t]\end{aligned}$$

Thus, back to (2):

$$\forall (x,y)\in\mathbb{R}^2, \quad |f_H^\tau(x,y) - t^2|y|^{1/H}|x|^{1/H}| \leq C\frac{2}{H}|x|^{1/H}[|x|^{1/H}+|y|^{1/H}][\epsilon^{2-2H}t^2+\epsilon t]$$

Now if we integrate with respect to the Gaussian density and coming back to (1), we obtain :

$$\begin{aligned}|\mathbb{E}(Var^\tau_{\frac{1}{H}}(B^H)^2) - t^2V_H^{1/H}\mathbb{E}(|N|^{\frac{1}{H}})^2| &= \left|\frac{1}{2\pi}\int_{\mathbb{R}}\int_{\mathbb{R}} e^{-\frac{(x^2+y^2)}{2}}[f_H^\tau(x,y) - t^2|y|^{1/H}|x|^{1/H}]dx\,dy\right| \\ &\leq \frac{1}{2\pi}\int_{\mathbb{R}}\int_{\mathbb{R}} e^{-\frac{(x^2+y^2)}{2}} C\frac{2}{H}|x|^{1/H}[|x|^{1/H}+|y|^{1/H}][\epsilon^{2-2H}t^2+\epsilon t]dx\,dy \\ &= \underbrace{[\epsilon^{2-2H}t^2+\epsilon t]\times \underbrace{C\frac{2}{H}\frac{1}{2\pi}\int_{\mathbb{R}}\int_{\mathbb{R}} e^{-\frac{(x^2+y^2)}{2}}|x|^{1/H}[|x|^{1/H}+|y|^{1/H}]dx\,dy}_{C'<+\infty}}_{=:g(\epsilon)}\end{aligned}$$

and $2-2H>0$.
To conclude, for any $\epsilon>0$, we have found a $\delta=\epsilon^2>0$ such that if the mesh is lower that δ, then $|\mathbb{E}(Var^\tau_{\frac{1}{H}}(B^H)^2) - t^2V_H^{1/H}\mathbb{E}(|N|^{\frac{1}{H}})^2|$ is lower than $g(\epsilon)$ which goes to 0 as $\epsilon\to 0$ which is the convergence we wanted. □

Technical lemma : LetB^H a fractional Brownian motion with Hurst parameter $H\in]0,1[$. There exists a continuous function R on $[-\frac{1}{4},\frac{1}{4}]^2$ and a constant C^H such that:

$$|R(x,y)| \leq C\min(|x|,|y|)^3|x|^{-H}|y|^{-H}$$

and for any (s,t,u,v) non negative real numbers such that $\max(\frac{|u|}{|t-s|},\frac{|v|}{|t-s|})\leq\frac{1}{4}$, one has :

$$\frac{\mathbb{E}([B^H_{s+u}-B^H_s][B^H_{t+v}-B^H_t])}{u^Hv^H} = H(1-2H)\left|\frac{u}{|t-s|}\frac{v}{|t-s|}\right|^{1-H} + R\left(\frac{u}{t-s},\frac{v}{t-s}\right)$$

Proof. First let :

$$\begin{aligned}
F(s,t,u,v) &:= \frac{\mathbb{E}([B^H_{s+u} - B^H_s][B^H_{t+v} - B^H_t])}{u^H v^H} \\
&= \frac{V_H}{2}\Bigg[|s+u|^{2H} + |t+v|^{2H} - |(t+v)-(s+u)|^{2H} \\
&\quad + |s|^{2H} + |t|^{2H} - |s-t|^{2H} \\
&\quad - (|s|^{2H} + |t+v|^{2H} - |(t+v)-s|^{2H}) \\
&\quad - (|t|^{2H} + |s+u|^{2H} - |(s+u)-t|^{2H}) \Bigg] \\
&= \frac{V_H}{2}[|s+u-t| + |s-v-t|^{2H} - |t-s|^{2H} - |t+v-s-u|^{2H}]
\end{aligned}$$

Set $x = \frac{u}{t-s}$ and $y = \frac{v}{t-s}$ to obtain :

$$\begin{aligned}
F(s,t,u,v) &= \frac{x^{-H}y^{-H}}{2}[|1-x|^{2H} + |1+y|^{2H} - 1 - |1+x-y|^{2H}] \\
&= \frac{x^{-H}y^{-H}}{2}\Bigg[\Big(1 - 2Hx + H(2H-1)x^2 + O(x^3)\Big) \\
&+\Big(1 + 2Hy + H(2H-1)y^2 + O(y^3)\Big) - 1 \\
&-\Big(1 + 2Hy - 2Hx + H(2H-1)(y-x)^2 + O((y-x)^3)\Big)\Bigg] \\
&= -H(2H-1)x^{1-H}y^{1-H} + \frac{x^{-H}y^{-H}}{2}\Big[O(x^3) + O(y^3) + O((y-x)^3)\Big] \\
&= -H(2H-1)x^{1-H}y^{1-H} + \Big[O(x^3) + O(y^3) + O(x^2y) + O(xy^2)\Big] \\
&= -H(2H-1)x^{1-H}y^{1-H} + O\Big((x^2+y^2)^{\frac{3}{2}}\Big)
\end{aligned}$$

□

Theorem 14 : Cholesky decomposition

Proof. For more clarity, let's denote $A_{i,j}$ the matrix obtained by deleting the i^{th} line and j^{th} column of a given matrix A and if $r \in \{1, \dots, n\}$, denote A_r the principal submatrix of order r. To prove the theorem, one requires the following tool :

lemma 2. *We call a lower-upper (LU) decomposition a decomposition of a matrix in a product LU where L is a lower and B an upper triangular matrix. A sufficient condition for an invertible matrix A to have a LU decomposition is to have all its principal minors to be different from zero. The decomposition is unique.*

Proof. (lemma) Let's prove the existence by an induction over n the dimension where the case $n = 1$ is immediate.
Let $n > 1$. Consider first for example that $A = \begin{pmatrix} A_{n,n} & b \\ b' & a \end{pmatrix}$. Note that $a \in \mathbb{R}$, $b, b' \in \mathbb{R}^{n-1}$.

$A_{n,n}$ is invertible and by hypothesis, all its minors are non zero, so there exists an $A_{n,n} = L'U'$ decomposition. We are thus looking for :

$$L = \begin{pmatrix} L' & 0 \\ v & l \end{pmatrix} \qquad U = \begin{pmatrix} U' & w \\ 0 & u \end{pmatrix}$$

with l imposed to be non zero and A=LU, that is :

$$A = \begin{pmatrix} L'U' & L'w \\ vU' & vw + lu \end{pmatrix}$$

equivalently :

$$\begin{cases} L'w = b \\ vU' = b' \\ vw + lu = a \end{cases}$$

from which one obtains a unique solution for w, v and u.
Let's prove now the unicity. Suppose $A = LU = L'U'$ with diagonal coefficients of L and L' to be equals and different from zero. Because matrices are trigonals one obtains $L^{-1}L' = UU'^{-1}$ and from what we imposed, these are equal to unity matrix which yields equality. □

Let's prove first that principal minors of $\Sigma \in \mathcal{S}_n^{++}(\mathbb{R})$ are different from zero and even positive. Let $r \in \{1, \dots, n\}$. Σ_r is symmetrical. Moreover, for any non zero $x \in \mathbb{R}^n$, $x\Sigma x^T > 0$. Therefore, for any non zero $x' \in \mathbb{R}^r$, complete x' with zeros into a non zero vector x of dimension n to obtain:

$$x'\Sigma_r x'^T = x\Sigma x^T > 0$$

Hence, Σ_r is positive semi-definite and its determinant is strictly positive.
Therefore, from lemma, Σ has an LU decomposition. There exists 3 unique matrices $L, D, U \in \mathcal{M}_n(\mathbb{R})$ with L a lower triangular matrix with unity diagonal, U an upper triangular matrix with unity diagonal, and D a diagonal matrix with positive coefficients such that :

$$\Sigma = LDU$$

By symmetry :

$$\Sigma = \Sigma^T = U^T D L^T$$

and by unicity of the decomposition, $U^T = L$. Setting $T := D^{\frac{1}{2}}U$, we obtain the Cholesky decomposition of Σ. □

B Python code : simulation of fractional Ornstein Uhlenbeck

```
import numpy as np
import pandas as pd
from scipy.fftpack import fft, ifft
from scipy.stats import norm
```

```
import matplotlib.pyplot as plt

def efficient_sim_GaussianVector(m,mu,c):
    n=c.size-1
    gamma=np.zeros(2*n)
    gamma[:n+1]=c
    gamma[n+1:]=np.flip(c[1:-1])
    lambd=fft(gamma)

    if np.any(lambd < 0):
        raise ValueError("The covariance function is not positive definite.")

    res=[]
    for i in range(m):
        Z=ifft(norm.rvs(size=2*n))
        X=fft(np.dot(np.diag(np.sqrt(lambd)),Z))
        res.append(X[:n]+mu)
    return res

def sim_fBm(H,n,delta,m):
    c=np.array([0.5*(abs(k+1)**(2*H)+abs(k-1)**(2*H))-abs(k)**(2*H) \
        for k in range(n+1)])
    mu=np.zeros(n)
    dX=efficient_sim_GaussianVector(m,mu,c)
    res=[]
    for k in range(m):
        vect=[]
        for j in range(n):
            vect.append(dX[k][:j])
            res.append((delta**H)*np.sum(vect[j]))
    #delete imaginary part since they all equal 0.
    eps = 1e-10
    res=np.array(res, dtype=complex)
    all_reals = np.all(abs(res.imag) < eps)
    if all_reals:
        res=res.real
    else:
        print("Error")
    return res

plt.figure()

n=500
delta=1/n
H=[0.2,0.5,0.8]
m=1
for i in range(3):
    W=sim_fBm(H[i],n,delta,m)
    plt.subplot(3,1,i+1)
```

```
    plt.plot(W,label="H={}".format(H[i]))
    plt.legend(loc='lower right')

def sim_fOU(H,n,delta,mu,nu,alpha,X0):

    # H the Hurst parameter
    # n the number of steps
    # delta the step size
    # mu the mean
    # nu the noise
    # alpha the reversion spead
    # X0 the initial value

    W=sim_fBm(H,n,delta,1)
    X=[X0]
    for step in range(1,n):
        X.append(X[step-1]+nu*(W[step]-W[step-1])+alpha*delta*(mu-X[step-1]))
    return X

### Plot log m(q,delta)

n=3540
delta=1
H=0.14
mu=-5
nu=0.3
alpha=5E-4
X0=-5

logvol=sim_fOU(H,n,delta,mu,nu,alpha,X0)
logvol=pd.Series(data=logvol)

def hurst_est(q, x, data):
    return [np.mean(np.abs(data - data.shift(lag))**q) for lag in x]

plt.figure(figsize=(7, 7))
plt.xlabel('$log(\Delta)$')
plt.ylabel('$log\, m(q,\Delta)$')
plt.ylim=(-3, -.5)

zeta_q = []
Q = np.array([.5, 1, 1.5, 2, 3])
x = np.arange(1, 100)
for q in Q:
    plt.plot(np.log(x), np.log(hurst_est(q, x,logvol)), 'x')
    model = np.polyfit(np.log(x), np.log(hurst_est(q, x, logvol)), 1)
    plt.plot(np.log(x), np.log(x) * model[0] + model[1], label="q={}".format(q))
    plt.legend(loc='lower right')
    zeta_q.append(model[0])
```

```
print(zeta_q)

### Plot simulated volatility

plt.figure()

# 3500 days, 1 data per day
n=3500
delta=1
H=0.14
mu=-5
nu=0.3
alpha=5E-4
X0=-5
logvol=sim_fOU(H,n,delta,mu,nu,alpha,X0)
logvol=pd.Series(data=logvol)
plt.plot(logvol.apply(np.exp),linewidth=0.3)
```

C Python code : Analysis of Oxford-Man Institute's data

```
import numpy as np
import pandas as pd
import matplotlib.pyplot as plt
import warnings

warnings.filterwarnings('ignore')

#Preparing data

df=pd.read_csv("./Documents/oxfordmanrealizedvolatilityindices.csv")
df.shape
title=df.iloc[1]
title=title.tolist()

for indice in range(20):
    var_name="n_index_"+str(indice+1)
    globals()[var_name]=[title[0]]+title[indice*19+1:(indice+1)*19+1]
data=df.drop([0,1],axis=0)
data.columns=title

def drop_columns(data, indice):
    first_col = data.columns[0]
    keep_cols = [first_col] + list(data.iloc[:, \
        indice*19+1:(indice+1)*19+1].columns)
    return data[keep_cols]

for indice in range(20):
    var_name="index_"+str(indice+1)
```

```
    globals()[var_name]=drop_columns(data, indice)

### Replicate graphs of the article for S&P 500 index

#preparing the table
row_max=index_1.loc[index_1['DateID']==20140331].index[0]
sp_rep=index_1.drop(index=range(row_max+1, len(index_1)+1))
sp_rep['SPX2.rk'] = pd.to_numeric(sp_rep['SPX2.rk'], errors='coerce')
sp_rep=sp_rep.dropna(subset=['SPX2.rk'])
logvol=sp_rep['SPX2.rk'].apply(lambda x: np.log(np.sqrt(x)))
logvol=logvol.reset_index(drop=True)

#Plot log m(q,delta)

def hurst_est(q, x, data):
    return [np.mean(np.abs(data - data.shift(lag))**q) for lag in x]

plt.figure(figsize=(7, 7))
plt.xlabel('$log(\Delta)$')
plt.ylabel('$log\ \ m(q,\Delta)$')
plt.ylim=(-3, -.5)

zeta_q = []
Q = np.array([.5, 1, 1.5, 2, 3])
x = np.arange(1, 100)
for q in Q:
    plt.plot(np.log(x), np.log(hurst_est(q, x,logvol)), 'x')
    model = np.polyfit(np.log(x), np.log(hurst_est(q, x, logvol)), 1)
    plt.plot(np.log(x), np.log(x) * model[0] + model[1], label="q={}".format(q))
    x_text = np.log(x[0])
    y_text = np.log(hurst_est(q, x, logvol))[0]

    # Afficher la valeur de la pente sur le graphique
    plt.text(x_text, y_text, 'Slope = {:.3f}'.format(model[0]), \
        fontsize=12, color='red')
    plt.legend(loc='lower right')

    zeta_q.append(model[0])

print(zeta_q)

#Plot zeta_q

Q=np.linspace(0,3,20)
zeta_q=[]
for q in Q:
    model = np.polyfit(np.log(x), np.log(hurst_est(q, x, logvol)), 1)
    zeta_q.append(model[0])
```

```
plt.ylabel('$\zeta_q$')
plt.xlabel('$q$')
plt.plot(Q,zeta_q,label="zeta_q")
plt.plot(Q,0.142*Q,label="0.142q")
plt.legend(loc='lower right')

#Plot log-volatility increments

from scipy.stats import norm

logvol=sp_rep['SPX2.rk'].apply(lambda x: np.log(np.sqrt(x)))
logvol=logvol.reset_index(drop=True)
lags=[1,5,25,125]
plt.figure(figsize=(15, 7))
for i in range(4):
    data=logvol-logvol.shift(lags[i])
    mu, std = norm.fit(data.dropna())
    plt.subplot(2,2,i+1)
    plt.title("$\Delta$={} day(s)".format(lags[i]))
    plt.hist(data,color='blue',density=True, bins=40,histtype='bar',alpha=0.5)
    x = np.linspace(-2, 2, 100)
    p = norm.pdf(x, mu, std)
    plt.plot(x, p, color='r', linewidth=2)

### Compare log-volatility smoothness over the different
### indexes on the same time interval (01/03/2000 up to 03/31/2014)

row_max=index_1.loc[index_1['DateID']==20140331].index[0]

L=pd.DataFrame(index=['zeta_0.5/0.5','zeta_1','zeta_1.5/1.5','zeta_2/2','zeta_3/3'])
Q=np.array([.5, 1, 1.5, 2, 3])
x = np.arange(1, 100)

for indice in range(20):

    zeta_q=[]
    index_nb="index_"+str(indice+1)
    var_name="logvol_index_"+str(indice+1)
    globals()[var_name]= \
        (globals()[index_nb]).drop(index=range(row_max+1, len(index_1)))
    (globals()[var_name]).iloc[:,1] = \
        pd.to_numeric((globals()[var_name]).iloc[:,1], errors='coerce')
    globals()[var_name]= \
        (globals()[var_name]).dropna(subset=[(globals()[var_name]).columns[2]])
    globals()[var_name]= \
        globals()[var_name].iloc[:,1].apply(lambda x: np.log(np.sqrt(x)))
    globals()[var_name]= \
        globals()[var_name].reset_index(drop=True)
    for q in Q:
```

```
        model = np.polyfit(np.log(x), \
                np.log(hurst_est(q, x, globals()[var_name])), 1)
        zeta_q.append(model[0]/q)
    L["{}".format(var_name)]=zeta_q

print(L.transpose())

### Plot volatility time series
plt.axis(ymax=0.06)
plt.plot(sp_rep['SPX2.rk'].apply(np.sqrt),linewidth=0.3)

### Further analysis : GFC

index_1['DateID'] = pd.to_datetime(index_1['DateID'], format='%Y%m%d')

r_start=index_1.loc[index_1['DateID'] == \
        pd.to_datetime('20070629', format='%Y%m%d')].index[0]
r_end=index_1.loc[index_1['DateID'] == \
        pd.to_datetime('20101231', format='%Y%m%d')].index[0]

sp_gfc=index_1.drop(index=range(2,r_start))
sp_gfc=sp_gfc.drop(index=range(r_end+1,len(index_1)+2))
sp_gfc['SPX2.rk'] = pd.to_numeric(sp_gfc['SPX2.rk'], errors='coerce')
sp_gfc=sp_gfc.dropna(subset=['SPX2.rk'])

logvol3=sp_gfc['SPX2.rk'].apply(lambda x: np.log(np.sqrt(x)))
logvol3=logvol3.reset_index(drop=True)

plt.figure(figsize=(7, 7))
plt.xlabel('$log(\Delta)$')
plt.ylabel('$log\␣␣m(q.\Delta)$')
plt.ylim=(-3, -.5)

zeta_q = []
Q = np.array([.5, 1, 1.5, 2, 3])
x = np.arange(1, 100)
for q in Q:
    plt.plot(np.log(x), np.log(hurst_est(q, x,logvol3)), 'x')
    model = np.polyfit(np.log(x), np.log(hurst_est(q, x, logvol3)), 1)
    plt.plot(np.log(x), np.log(x) * model[0] + model[1], label="q={}".format(q))
    plt.legend(loc='lower␣right')
    zeta_q.append(model[0])


Q=np.linspace(0,3,20)
zeta1_q=[]
zeta2_q=[]
x = np.arange(1, 100)
for q in Q:
```

```
    model1 = np.polyfit(np.log(x), np.log(hurst_est(q, x, logvol)), 1)
    zeta1_q.append(model1[0])
    model2 = np.polyfit(np.log(x), np.log(hurst_est(q, x, logvol3)), 1)
    zeta2_q.append(model2[0])

plt.figure(figsize=(7, 7))
plt.ylabel('$\zeta_q$')
plt.xlabel('$q$')
plt.plot(Q,zeta1_q, label="2000-2014")
plt.plot(Q,zeta2_q, label="2007-2010")
plt.legend(loc='lower right')
```

References

[1] F. Comte and E. Renault. Long memory in continuous-time stochastic volatility models. 1998.

[2] Laure Coutin. An introduction to (stochastic) calculus with respect to fractional brownian motion.

[3] Laurent Decreusefond and Ali Suleyman Üstünel. Fractional brownian motion: Theory and applications. Vol.5, 1998.

[4] B. Dupire. Pricing with a smile. 1994.

[5] M. Fukasawa. Asymptotic analysis for stochastic volatility: Martingale expansion. 2011.

[6] J. Gatheral and R. C. Oomen. Zero-intelligence realized variance estimation. 14(2):249-283, 2010.

[7] Paul P. HAGER. Exercise sheet - simulation of fractional brownian motion. 2022.

[8] S. L. Heston. A closed-form solution for options with stochastic volatility with applications to bond and currency options. 1993.

[9] J. Hull and A. White. One-factor interest-rate models and the valuation of interest-rate derivative securities. 1993.

[10] Mathieu Rosenbaum Jim Gatheral, Thibault Jaisson. Volatility is rough. 2014.

[11] Mikko S. Pakkanen Mikkel Bennedsen, Asger Lunde. Decoupling the short- and long-term behavior of stochastic. 2021.

[12] Ivan Nourdin. Selected aspects of fractional brownian motion. 2012.

[13] A. S. Lesniewski P. S. Hagan, D. Kumar and D. E. Woodward. Managing smile risk. 2002.

[14] Makoto Maejima Patrick Cheridito, Hideyuki Kawaguchi. Fractional ornstein-uhlenbeck process. Vol. 8, 2003.

[15] Thierry Lévy Terry J.Lyons, Michael J.Caruana. Differential equations driven by rough paths. 2004.

[16] Mathieu Rosenbaum Thibault Jaisson. Rough fractional diffusions as scaling limits of nearly unstable heavy tailed hawkes processes. 2015.

[17] Richard L. Wheeden and Antoni Zygmund. Measure and integral: An introduction to real analysis.

Mes remerciements à M. Delarue pour ses conseils et sa bienveillance.
Mes remerciements à M. Pelgrin pour son encadrement.